THE MINERALISATION AND GEOLOGY OF THE PATAWARTA DIAPIR NORTHERN FLINDERS RANGES, SOUTH AUSTRALIA.

By

David Hall, B.Sc.

Submitted as partial fulfilment of the Honours Degree
of Bachelor of Science in Geology,
at the University of Adelaide,
November, 1984.

National Grid Reference SH 549-6638 (1:100,000)

View of Patawarta Diapir looking
north east towards Patawarta Gap

CONTENTS

CONTENTS (Continued)

APPENDICES

TABLES

FIGURES

PLATES

ABSTRACT

The Patawarta Diapir is located in the northern Flinders Ranges, approximately 17 km north-east of Blinman. It has intruded into the late Proterozoic Wilpena Group sediments of the Adelaide Geosyncline. The elements occurring within the diapir consist of disrupted blocks of a variety of rock types, most of which can be correlated with rocks of Willouran age. The blocks are enclosed by a matrix of carbonate breccia.

Widespread Cu mineralisation is present in the diapir, mainly as epigenetic veins. Anomalous levels of Zn, Pb, As, Co and Ni are also found in rock chips and stream sediment samples.

Fluid inclusion data for quartz suggest a temperature of formation of the veins of approximately 150°C. Freezing point determinations indicate greater than 20 wt % NaCl equivalent on average.

Sulphur isotope studies suggest that sulphur in the mineralisation was essentially derived from evaporites, but a small contribution may have come from a mafic igneous source.

Origin of the mineralising brines is postulated to be through compaction of Callanna Bed sequences and leaching of base metals from Adelaidean (and possibly basement) rocks. Reduced sulphur and base metals are interpreted to have travelled together in the same brine and precipitation occurred in open fractures in the diapir.

1. INTRODUCTION

1.1 Location and Physiography

The Patawarta Diapir lies in rugged country on Mooloolоo Station, 17 km north-east of Blinman, in the Northern Flinders Ranges. It is located at latitude 30° 56' 05", longitude 138° 40' 00" on the Copley 1:250,000 field sheet. Mooloolоo Station is 15 km north of Blinman and the diapir is located 12 km north east of the homestead. The study area lies in a class B environmental zone (Figure 1). Access to the diapir is only possible using four-wheel-drive vehicles.

The diapir is well vegetated, supporting stunted growths of erenomophilia and salt bush with sparse larger eucalypts in the carbonate lithologies, while native pines are abundant in the siltstone and shale lithologies. Surface water is available only in good seasons and only one water bore occurs in the area (Pendulum Well). The diapir shows a complex drainage pattern which accentuates the general, moderate exposure of the lithologies.

1.2 Aims

The aims of this project were to map and describe the geology of the Patawarta Diapir and to investigate the mineralisation of the area, using mineralogical and chemical data, fluid inclusion measurements and sulphur isotope studies. This information is used to discuss probable geologic processes which led to the formation of the mineralised veins in the diapir.

1.3 Previous Investigations

To date, most reports on the Patawarta Diapir have concentrated on the economic prospects of the region. The first report from the

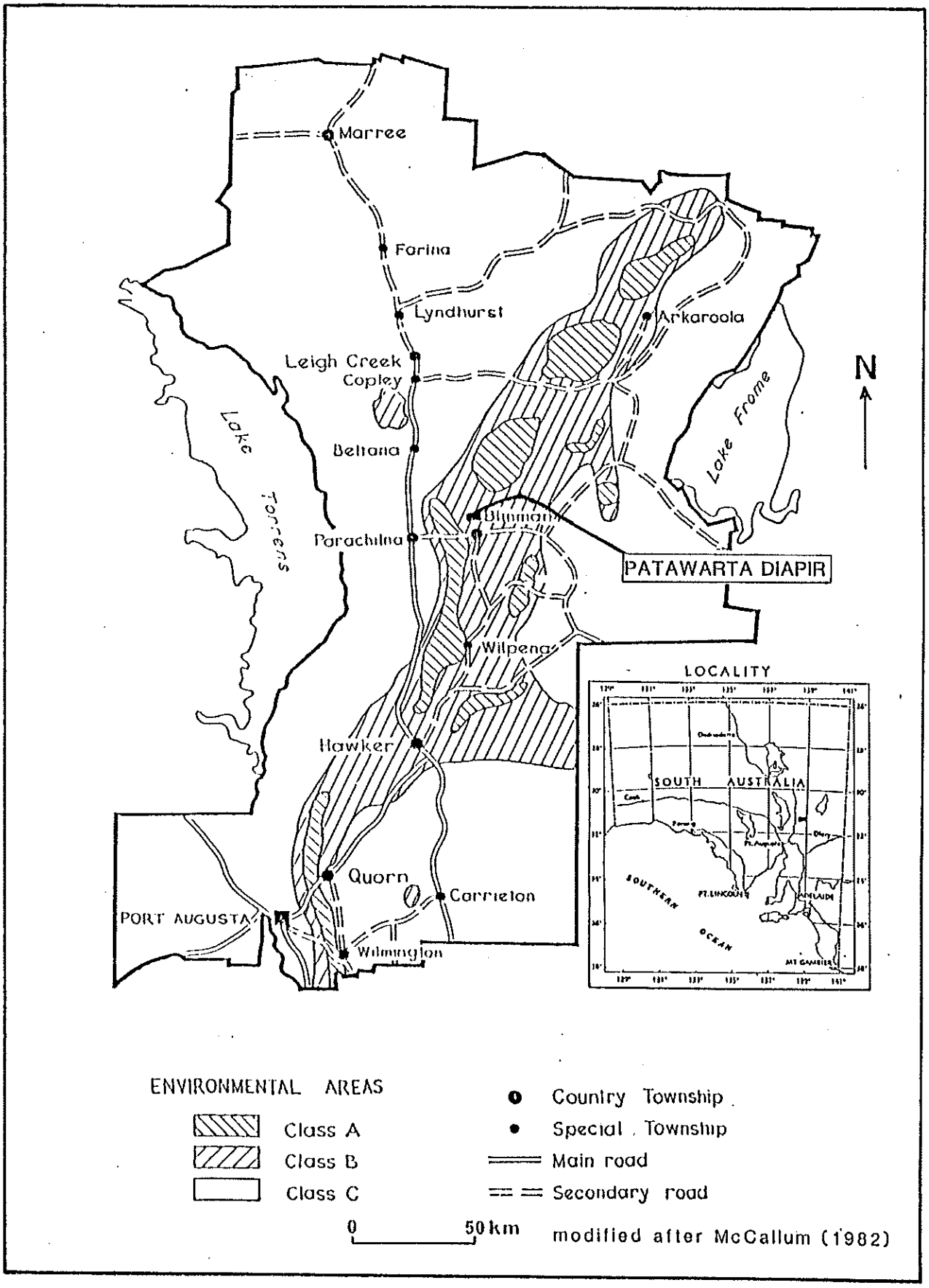

FIGURE 1 Locality Map

area was undertaken by Austin (1863), who recorded Cu ore with a high Bi content from the Mount Rugged workings. The Inspector of Mines (1901) reported Cu ores with Au contents up to 53 g/tonne from the Mosley's workings (in Brown, 1908).

Dickinson (1944) described the Lady Lehmann workings and based on the Cu assay results concluded that the vein was uneconomic. Admin Exploration drilled 13 percussion holes along the line of the Lady Lehmann workings (Shackleton, 1968).

Read (1971) carried out a stream sediment survey for base metals on behalf of North Flinders Mines. He recorded no unusual anomalies except for Cu which was associated with known Cu occurrences.

Golding (1983) reinvestigated the major mineral occurrences of the diapir for E.Z. Exploration and currently E.Z. are still undertaking work in the area.

2. GEOLOGICAL SETTING

2.1 General

The term 'diapir' is an Anglo-derivation of the Greek word 'diapeiren' which means "to pierce". O'Brien (1968) has defined diapirism as "a process in which earth materials from deeper levels have pierced, or appear to have pierced shallower materials". The term is applied to physical emplacement of mainly sedimentary material at low temperatures.

The Patawarta Diapir was introduced along the Narina Fault Zone (Coates 1973) where the fault trends west-north-west, producing an elongate structure. Callen (1970) regarded the Narina Fault as a vertical strike slip fault and suggested that the Patawarta Diapir intruded and filled spaces caused by opening up along the western end of the fault where it splits into a "horsetail zone consisting of several short curved faults".

The diapir is elongated in a west-north-west, east-south-east orientation parallel to the strike of the host Adelaidean sediments which dip generally north-eastwards.

2.2 Host Rock Lithology

The Patawarta Diapir has been intruded into host sedimentary rocks comprising shales, siltstones, limestones and quartzites of the late Proterozoic Wilpena Group (Figure 2). The oldest rocks intruded by the diapir are the red and purple shales of the Bunyeroo Formation. These are overlain by the green-grey calcareous shales and grey sandy limestones of the Wonoka Formation. The Wonoka Formation is overlain by the Pound Quartzite, a white cross bedded and ripple marked feldspathic quartzite which forms a prominent ridge running in a northwest direction.

The ABC Range Quartzite, a white ripple marked sandy quartzite, together with the purple flaggy siltstones of the Brachina Formation, both stratigraphically underlie the Bunyeroo Formation, all of which have been folded around so that they lie in contact with the northwest portion of the diapir.

The regional dip of the host rocks, produced by the Delamerian Orogeny is approximately 25° to the northeast.

2.3 Geology of the Diapir

The elements occurring within the core of the diapir consist of disrupted blocks of a great variety of rock types, including calcareous siltstones and shales, limestones, sandstones and igneous rocks, enclosed by a matrix of brecciated sediment (Figure 2). These blocks or "rafts" show great variation in size with the largest having a length of over 2 km and many are overturned. Detailed thin section descriptions of the diapiric lithologies are given in Appendix 1.

2.3.1. Sedimentary Lithologies

The major sedimentary lithologies recognised in the diapir are as follows:

(i) Heavy mineral laminated sandstone and quartzite.

This unit is characterised by cross bedding and ripple marks. The sandstones are fine to coarse grained and contain quartz, feldspar, coarse detrital mica and abundant hematite. Bedding ranges from 1 cm thick up to 1 m thick. The coarsest beds are best interpreted as the result of storm activity and were laid down very quickly as indicated by flat laminations and minor graded bedding in the poorly sorted sands. Finer sand beds show small scale cross bedding, ripple marks and load casts. Cross bedding indicates that several of these rafts are overturned. Halite casts, ranging from 2 to 10 mm, are present in thinner beds of siltstone occurring with the sandstones.

(ii) Calcareous and dolomitic siltstone and shale.

This is the most common lithology in the diapir and comprises grey-green calcareous siltstone and shale which are dolomitic in part. These sediments are characterised by abundant halite casts showing hopper face morphology and cubic form. Gypsum pseudomorphs are also recognised but are not nearly as common as halite casts. Other sedimentary features are heavy mineral laminations, minor slump folds, casts of mud cracks and load casts. Disseminated fine grained hematite is very common and its distribution and variation in grain size suggest that it is of detrital, sedimentary origin.

(iii) Interbedded sandstone, siltstone and sandstone.

Micaeous and feldspathic, fine to coarse grained sandstones are interbedded on a centimetre scale with calcareous siltstone and shale. Halite casts and heavy mineral laminations are common.

(iv) Black limestone.

Thinly bedded black limestones occur in association with calcareous siltstone and shale. This unit is intensely folded in part and may indicate deposition in an environment with episodic tectonic instability since the surrounding siltstones are undeformed.

(v) Dolomite.

Dolomite rafts occurring in the diapir include both bedded and massive types and are generally weakly brecciated. Many small dolomite rafts are incorporated in the carbonate breccia and are too small to be mapped. They contain halite casts and gypsum pseudomorphs (Plate 2).

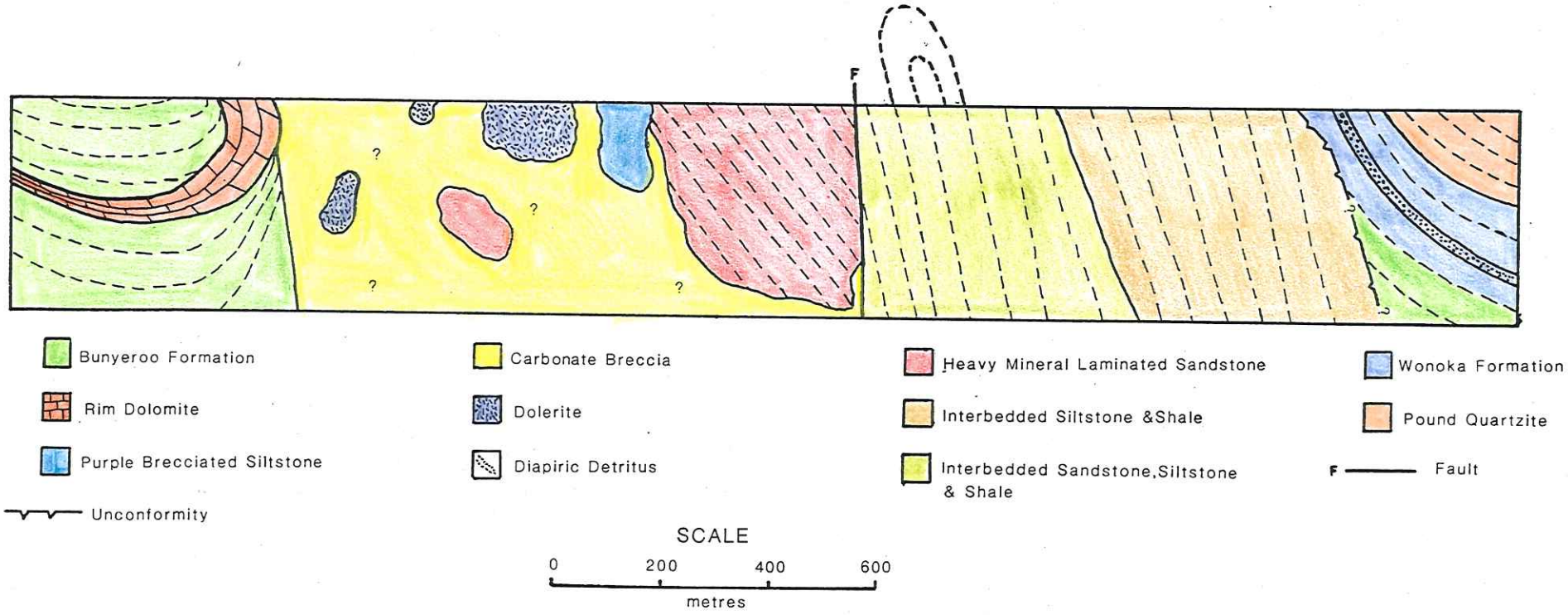

FIGURE3 INTERPRETIVE CROSS SECTION THROUGH PATAWARTA DIAPIR

(vi) Rim Dolomite.

An unusual formation in the study area is the Rim Dolomite so named by Read (1971). This lithology outcrops along the southwest rim of the diapir and is a prominantly outcropping carbonate rock. It contains numerous subrounded to subangular clasts of diapiric detritus and has a sedimentary bedded aspect. Red and white chert fragments are common and have been attributed to the breaking up of silica bands. (Read, 1971). Read has equated this dolomite with dolomites occurring on the margins of the Blinman Diapir and which Coates (1964) attributed to "metamorphic differentiation of dolomitic material from carbonate breccia" with the apparent bedding being interpreted as a flow structure developed during emplacement of the diapir.

This study suggests that the Rim Dolomite forms part of the Bunyeroo Formation. It cannot be a raft in the diapir since the red shales of the Bunyeroo Formation are conformable with the unit and no carbonate breccia is observed between the shales and the dolomite. The proposed mode of formation of the Rim Dolomite is shown in Figure 4. At the time of deposition of the dolomite bed, which is interpreted to be as a local facies of the Bunyeroo Formation, intrusion of the diapir commenced and as a sedimentary high, shed off diapiric rock fragments which were later incorporated in the dolomite. The clasts can be clearly recognised as belonging to lithologies contained within the diapir. The amount of rounding of the clasts reflects their degree of reworking before incorporation in the dolomite. Several minor phases of diapiric uplift may have occurred during deposition of the dolomite as indicated by irregular beds where clasts are abundant alternating with beds where clasts are rare. (Plate 1).

Diapirism is then inferred to have ceased until deposition of the Wonoka Formation. At this time uplift of the diapir recommenced and diapiric detritus was incorporated in the grey limestones of the Wonoka Formation along the northwest rim of the diapir (See Figure 2). This later movement caused an upturning and faulting of the Rim Dolomite and the red shales of the Bunyeroo Formation.

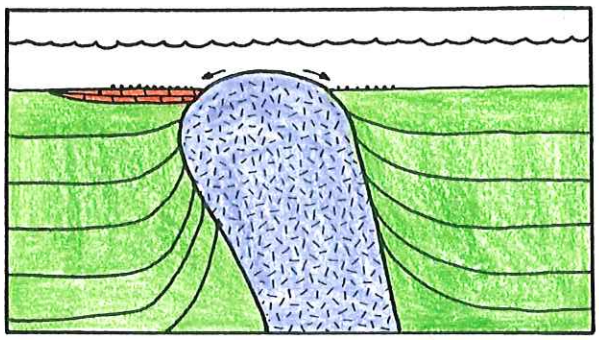

STAGE 1

Intrusion Of Diapir During "Bunyeroo Time"

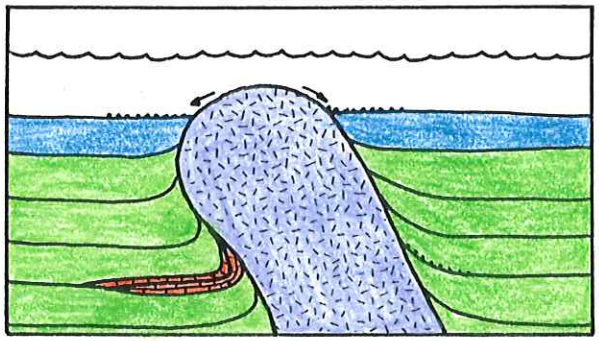

STAGE 2

Second Phase Of Movement During "Wonoka Time"

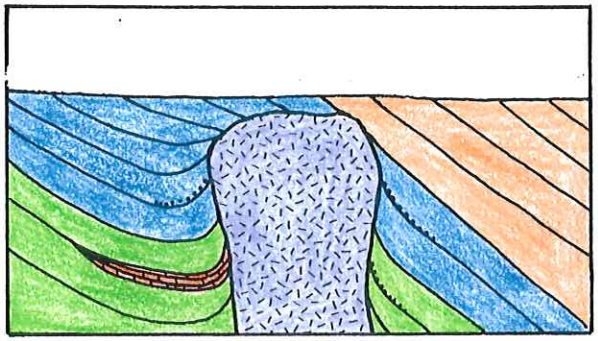

STAGE 3

Effect Of Delamerian Orogeny

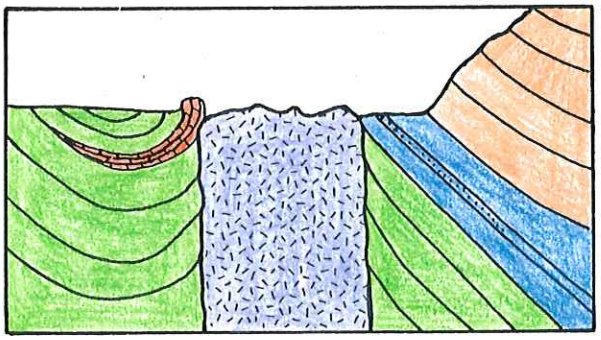

STAGE 4

Present Day

FIGURE 4 INFERRED STAGES OF FORMATION OF RIM DOLOMITE

Diapir | Rim Dolomite | Bunyeroo Formation | Diapiric Clasts

Wonoka Formation | Pound Quartzite | (not to scale)

Subsequent overprinting by the Delamerian Orogeny produced the regional dip of 25° to the north-east in the host rocks and the formation of an apparent syncline about the axis of upturning adjacent to the diapir (Figure 2).

In order to produce the almost vertical dip in the Rim Dolomite seen at the present day, the unit must have been overturned by about 25°, during the second major phase of diapiric movement. The Delamerian Orogeny would have had the effect of tilting the dolomite bed and adjacent shales to the dip seen today. Since intrusion of the diapir would produce steepening of the dolomite to vertical with only minor overturning, (N. Lemmon, pers. comm.), an element of thrusting during diapirism is inferred to produce the overturning required for the model. (Figure 4).

All sedimentary lithologies contained within the diapir show features of a shallow water to subaerial depositional environment. Most of these units can be correlated with units of the Lower Callanna Beds of the Willouran Series occurring elsewhere, in the Flinders Ranges, in stratigraphic sequence (Table 1).

Rowlands et al. (1980) have interpreted similar Callanna Bed sequences in the Willouran Ranges as forming in sabkha and playa environments.

2.3.2. Igneous Rocks.

In addition to the sedimentary rocks, mafic intrusive and extrusive rocks have been recognised.

The extrusive rocks are represented by fine grained dark green-grey amygdaloidal and non-amygdaloidal altered basalts. Two amygdaloidal basalts were noted and had vesicles predominantly filled with calcite although some amygdales included hematite and siderite. Thin sections show the basalts to consist of laths of plagioclase in a matrix of calcite, epidote, albite, chlorite, actinolite and abundant iron oxide. Coates (1964) noted similar rocks in the Blinman Diapir and suggested that these rocks were

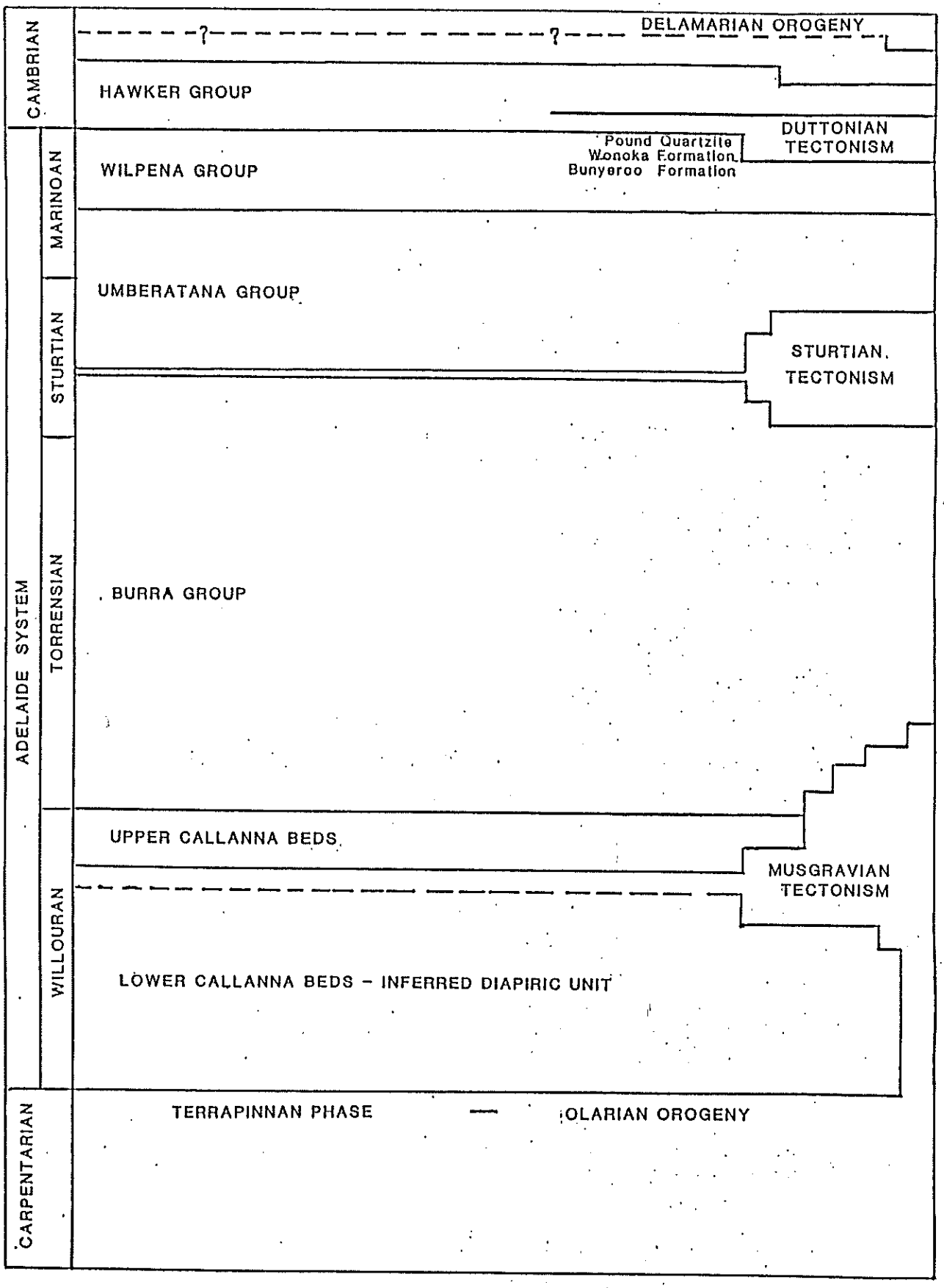

TABLE 1. PRECAMBRIAN STRATIGRAPHY IN THE NORTHERN PART OF THE ADELAIDE GEOSYNCLINE (MODIFIED AFTER PARKIN 1969).

not emplaced after diapiric intrusion but were fragments of volcanic rock equivalent to the Wooltana Volcanics of Willouran age. Whole rock analyses confirm the similarity of the extrusive rocks at Patawarta and those of Blinman and Wooltana (Table 2).

The intrusive rocks are represented by fine to medium grained dark green dolerites, almost identical in appearance to the non-amygdaloidal basalts. The dolerites are also altered with original laths of labradorite being decalcified and producing albite. Epidote and calcite are evident and Spry (1952), in a study of igneous rocks in the Worumba region, attributes this to the process of saussuritisation. Chlorite and minor amphibole (fibrous actinolite and riebeckite) are minor assemblages.

In two localities dolerites have caused local contact metamorphism of the surrounding shale and siltstone to hornfels but dolerites enclosed by carbonate breccia show a general absence of contact metamorphic effects. This may imply that the majority of dolerites in the diapir were dyke feeders for the basalts of Willouran age and now form diapiric xenoclasts. One locality in the south-west portion of the diapir suggests an intrusive relationship into Willouran sediments which were themselves subsequently disrupted. Whole rock analyses show the similarity of the intrusive and extrusive rocks (Table 2).

A contact metamorphic zone of chloritic marble would be expected if a dolerite was intruded post-diapirically into carbonate breccia. No evidence of this type of contact metamorphism has been noted in the Patawarta Diapir although reports of post-diapiric dolerites have been reported from other diapirs, (Preiss, 1980) implying a post Willouran phase of igneous activity in the Adelaide Geosyncline. On the other hand, none of the Patawarta dolerites show evidence of brecciation or dolerite fragments in the surrounding carbonate breccia, as would be expected if they were of Willouran age and subsequently intruded with the diapir.

It should be noted that the dolerites only occur within the diapiric core complex and not in the surrounding host rocks which may imply that the dolerites do not post date diapirism.

TABLE 2. GEOCHEMICAL ANALYSES OF BASALTS & DOLERITES

I Amydaloidal basalt, Patawarta Diapir

II Dolerite, Patawarta Diapir

III Basalt, Wooltana : Mawson (1926)

IV Basalt, Blinman Diapir; Coates (1964)

V Dolerite, Blinman Diapir; Coates (1964)

	I	II	III	IV	V
SiO_2	49.25	49.17	48.46	48.0	48.11
Al_2O_3	15.50	14.53	18.76	13.8	15.08
Fe_2O_3	13.24	15.19	6.38	12.1	4.73
FeO	Not det.	Not det.	3.01	2.80	8.37
MgO	6.08	7.59	6.94	6.45	5.87
CaO	9.37	7.31	5.00	4.80	9.75
Na_2O	3.42	3.28	3.44	4.60	3.33
K_2O	1.15	2.70	1.89	1.18	1.45
TiO_2	1.92	1.84	1.53	1.83	2.10
P_2O_5	0.19	0.16	0.28	0.21	Not det.
MnO	0.16	0.12	0.08	0.07	0.12
TOTAL	100.25	99.88	99.68	99.79	100.43

2.3.3. Diapiric Breccia.

The diapiric breccia is distinguished by its high carbonate content which consists essentially of dolomite with subordinate calcite. Approximately 60% of the breccia is made up of a wide variety of rock types varying in size from very small clasts (1 cm) up to large blocks of several metres. The rock fragments, comprising partly recrystallised siltstone, shale, sandstone, dolomite and quartzite, are cemented by a carbonate matrix of dolomite, calcite and minor quartz. Accessory constituents are specular hematite, talc, rutile, pyrite, limonite, microcline and siderite.

The reason for the high carbonate content in the breccia matrix is uncertain as it seems unlikely that the fractured and crushed calcareous beds from low down in the Adelaidean System would be a significant source for all the cementing carbonate.

PLATE 1

(a) Rim Dolomite, south west portion of diapir. Note bedded aspect

(b) Rim Dolomite, showing subrounded to subangular clasts of diapiric detritus, defining bedding

(c) Purple brecciated siltstone containing portions of brecciated basalt. Some original bedding can still be recognised

a

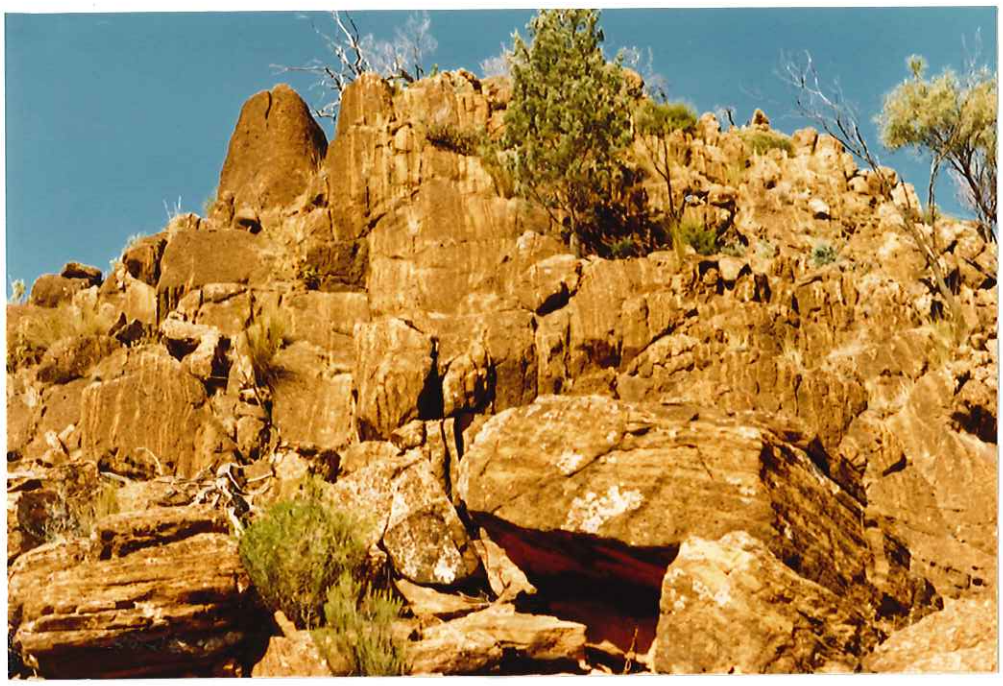

b

c

PLATE 2

(a) Basalt block sitting on top of a sedimentary breccia containing basalt clasts.

(b) Typical carbonate breccia.

(c) Halite casts and gypsum pseudomorphs in a dolomite raft.

a

b

c

PLATE 3

(a) Cross bedding in hematite -bearing siltstone. Much of the bedding is marked by concentrations of hematite (Transmitted light) (30x)

(b) Carbonate breccia showing interlocking dolomite grain and limonite staining (dark area) (Transmitted light) (40x)

(c) Altered amygdaloidal basalt

(d) Contact rock against a dolerite plug. The rock has recrystallised and the former sedimentary bedding is now shown only by concentrations of recrystallised hematite.

a

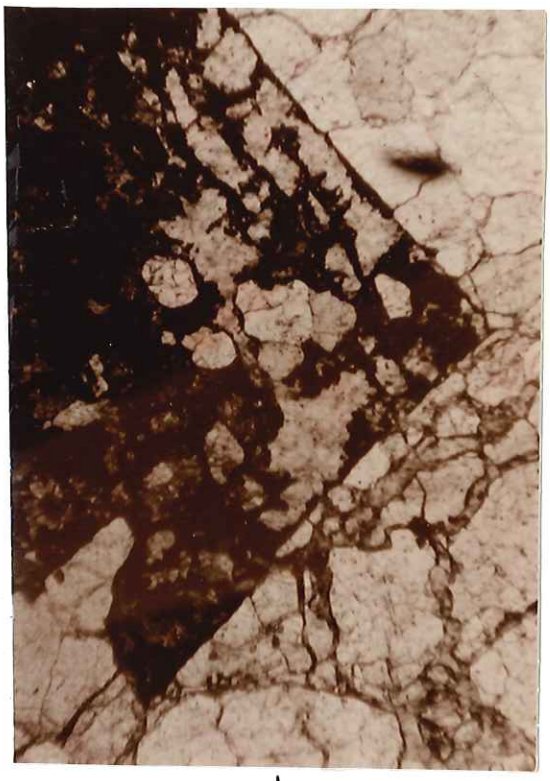

b

c

d

3. MINERALISATION

3.1 General

The widespread Cu mineralisation in the Patawarta Diapir appears to be patchy and is irregularly exposed (Figure 2). The mineralisation is of epigenetic type, characterised by narrow cross cutting veins of calcite, siderite and rarely hematite, containing pyrite, chalcopyrite and malachite. The veins occur in calcareous shales and siltstones which are often weakly brecciated. Cu is principally present as malachite and disseminated chalcopyrite in the veins. Cu is the major anomalous metal found in the diapir but anomalous levels of Zn, Pb, As, Co and Ni in various parts of the diapir are indicated by stream sediment sampling carried out by E.Z. Exploration.

In a few instances, minor sulphides occur with malachite in a stratiform fashion but it is doubtful that this was of syngenetic origin. Binks (1968) suggested that this was due to permeation of mineralising solutions along bedding planes with subsequent selective replacement of certain laminae.

The coarsely crystalline calcite and siderite veins show an orientation of approximately north-south with a variation of 45° either side.

Vein-type mineral occurrences are also present in the Rim Dolomite in the form of coarsely crystalline barite veins and thin 1 - 2 cm calcite veins containing minor sulphides and malachite.

3.2 Description of Major Mine Workings

There are 5 main groups of workings in the Patawarta Diapir plus various isolated pits, all of which show anomalous Cu values (Figure 2). These workings have been previously described by Read (1971) and Golding (1983).

3.2.1 Lady Lehmann Workings

In addition to Read (1971) and Golding (1983), this group of workings has also been described by Dickinson (1944) and Shackleton (1968). The lode comprises a massive calcite vein up to 1.5m wide, bearing grains of disseminated chalcopyrite and pyrite. The vein occurs at the contact between a raft of calcareous and dolomitic siltstone and diapiric breccia (Plate 4). Workings along the northern boundary of the siltstone raft would seem to indicate that the lode continues for about 700m but Dickinson reported that the lode was not continuous. Dickinson concluded that "the lode contained 1.7% Cu over an average width of 3' 6" with a tonnage yield of 100 - 150 tonnes per vertical foot."

Adit F shows excellent exposure of the calcite vein and the host rocks (Figure 5). Along this adit the calcite lode strikes 40° with almost vertical dip and is not conformable as the host siltstones strike 80°. The hanging wall siltstones are well defined and have a sharp contact with the lode. The vein gangue is made up of a mixture of both coarse grained and finer grained fibrous calcite with minor quartz and very occasional anhedral grains of albite.

The footwall rock is a diapiric carbonate breccia containing rock fragments of several types. Midway down the adit the breccia contains large clasts of pyritic black shales in which both fine grained and coarse grained pyrite are present. Pyrite is disseminated through both the breccias and the siltstones.

The calcite vein does not extend more than 1.5m from the hanging wall and shows variable thickness along the adit. Where the calcite pinches out the breccias are in direct contact with the siltstones. Slickensides pitching south-west at 50° occur in the hanging wall and Dickinson suggested that the vein thickness was controlled by "the varying degree of opening movements which took place along the hanging wall fissure". Golding suggested the form of the lode indicated "that hydrothermal solutions dammed up againt the siltstones after moving through the footwall breccia".

FIGURE 5 LADY LEHMANN MINE

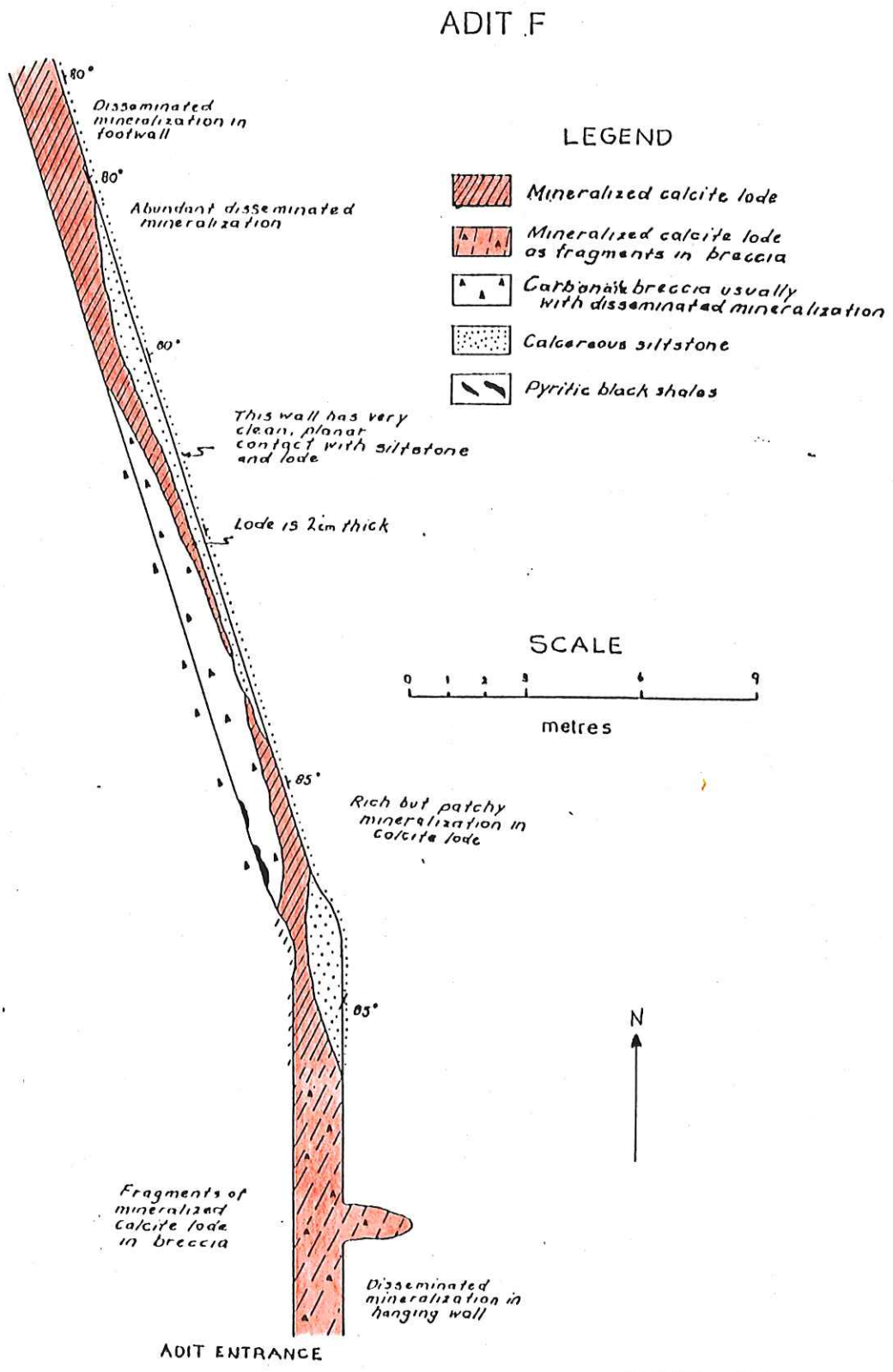

D. J. HALL 1984

(Adapted from W.G.Shackleton (1968))

The first 10m of the lode in the adit indicate that it was brecciated subsequent to emplacement as there is no continuity to the vein in this locality, although fragments of mineralised calcite lode occur in the footwall breccia.

Malachite staining is particularly predominant in the hanging wall siltstones and extends across the lode into the footwall breccia. The sulphide minerals have penetrated beyond the limits of the calcite vein into the breccia and although their concentration diminishes rapidly with increasing distance from the hanging wall, assay results indicate that the disseminated mineralisation in the breccia is comparable to that of the calcite lode in places.

Thin sections show the hanging wall siltstones to consist predominantly of quartz, orthoclase, sericite and calcite with minor quantities of hematite and chlorite and muscovite (Appendix 1). Alteration of the siltstones was apparently due to the highly saline brines which formed the lode and caused alteration of orthoclase to sericite (Appendix 1).

Other workings extend to the east along the northern edge of the siltstone raft and show similar mineralisation although the calcite lode is nowhere as well exposed as in adit F.

3.2.2. Lady Lennon Workings

These workings are sited on ferruginous calcite and siderite veins carrying minor amounts of disseminated chalcopyrite and pyrite, occurring in fractures in a calcareous siltstone raft over a distance of 600m. Malachite is the predominant Cu mineralisation and has diffused into the host siltstones. The main working consists of a small open cut with two short adits at different levels on the side of the hill. Thin veins of siderite, containing disseminated sulphides and malachite cut across the host siltstones. Gold has been reported from this locality and one sample of vein material yielded an average gold value of 28 ppm (Golding 1983).

Other workings in the group occur to the east of the main working and are sited on massive calcite veins up to 1m across. In all of these, malachite is contained along joint planes and bedding plane fractures in the adjacent siltstones.

3.2.3 Mosleys Workings

The Mosleys group of workings consists of a number of narrow costeans and pits in host rocks of grey-green calcareous siltstones and shales. The costeans follow Cu rich veins with specular hematite, ferruginous calcite and siderite varying up to a half metre in width, which cut through the host rocks in a general north-south orientation. Fractures in the siltstones are stained by malachite. These workings are characterised by the abundance of specular hematite. Brown (1908) reported up to 53 ppm Au from vein material taken from the 10 m deep main shaft but more recent assays have shown much lower gold values in the order of 5 ppm.

3.2.4 Home Rule Flat Workings

The Home Rule Flat Workings occupy an area with very little outcrop but, as with the other workings, the pits are sited on coarse grained calcite veins containing malachite and minor sulphides. The host rocks are calcareous shales and siltstones of a lithology similar to those at the Lady Lehmann and Lady Lennon workings. Gold has been reported from these diggings and in one polished section (831-126) one coarse grain of electrum (argentiferous gold) has been found (Plate 6).

3.2.5 Mount Rugged Workings

The two pits assumed to be the Mount Rugged workings are sited in the contact zone of a small dolerite plug. Hematite, pyrite, chalcopyrite and malachite are contained in a small calcite vein in contact metamorphosed breccia. Another pit in the vicinity is located in manganiferous rocks which, as well as showing anomalous Cu values, yielded very high Ni values (1.8%).

3.3 Mineralisation in the Igneous Rocks

The igneous rocks of the Patawarta Diapir do not show prominent Cu mineralisation, unlike those of other diapirs in the Flinders Ranges (eg. Blinman Diapir).

Only one dolerite occurrence, near the Mount Rugged Mine, showed characteristic malachite staining. Since this dolerite is sited very close to a sulphide bearing calcite vein the copper is likely to be derived from this vein rather than the dolerite. Analysis of four dolerite samples show extremely low values of Cu, Pb and Zn. (<1 ppm). Ni contents in the dolerites range up to 150 ppm which are not unexpected for a mafic rock (Rose et. al., 1979).

Basalts show only slightly higher values of Cu (up to 5 ppm) with Pb and Zn still being very low (<1 ppm). Malachite staining was noted in only two non amygdaloidal basalts in the study area. Ni contents range up to 50 ppm in amygdaloidal basalts and up to 70 ppm in nonamygdaloidal basalts.

3.4 Barite Veins

Three barite veins are present in the Rim Dolomite along the south-western margin of the diapir. These range in thickness from 0.5 up to 2 m in width. These veins have infilled small faults, presumably generated during formation of the diapir. The veins consist of coarsely crystalline barite with minor quartz and opaques and may have formed from the precipitation of barium sulphate from barium-saturated brine. No barite veins were noted within the core of the diapir suggesting that the formation of the barite veins and the sulphide bearing calcite veins were not related and presumably occurred at different times.

3.5 Mineral Descriptions and Textural Relationships

Examination of polished thin sections of the vein material shows the major sulphides are pyrite and chalcopyrite with grains ranging up to 5 mm in diameter. These are unevenly distributed throughout the gangue material and generally comprise less than 5% of the vein. Chalcopyrite typically comprises 60% of the total sulphides present. Small anhedral to subhedral grains of sphalerite are found in association with the major sulphides and most of the sphalerite is contained as inclusions within pyrite and chalcopyrite. This explains the zinc anomalies indicated through stream sediment sampling, by E.Z. Exploration. Other inclusions found within the major sulphides are calcite and very

occasional euhedral grains of marcasite. Chalcopyrite contains pyrite grains of varying sizes (Plate 5) and in some cases chalcopyrite appears to partially replace pyrite.

Secondary alteration effects are very noticeable in all samples. Subsequent to the emplacement of the sulphide bearing veins, weathering has resulted in the oxidation and leaching of the sulphide minerals and redistribution of much of the copper has occurred. Many of the sulphide grains have been replaced by limonite which is common in all samples. Limonite, when it has replaced the sulphides, shows a botryoidal texture which implies a rythmic replacement of the sulphides (Plate 6). Electron microprobe studies of limonite show up to 1% Cu dispersed through it and so much of the copper present may have been deposited from oxidising solutions of supergene origin.

Covellite and chalcocite, the products of supergene enrichment of copper ore, occur in association with chalcopyrite and to a minor extent with pyrite (Plate 5). Covellite coatings occur around the chalcopyrite grains and are more widespread than chalcocite. Both of these secondary sulphides occur as a compact mass of uniform fine polygonal grains. In one case covellite occurs in a cleavage crack in a larger sphalerite grain. Much of the copper is now present as malachite with very minor azurite; these oxidation products are to be expected in such a calcareous environment.

No arsenic minerals (eg. arsenopyrite) were noted in any of the thin sections and consequently the observed As anomaly in the area cannot be explained.

3.6 Mineral Chemistry of Selected Sulphides

Using the electron microprobe, samples of pyrite and chalcopyrite have been analysed for Co, Ni, Ti and As. Results are shown in Appendix 3. For pyrite, Co values are quite high, ranging from just over 1% down to 0.9%. Ni and Ti values are considerably lower, averaging about 30 ppm. As values range up to 200 ppm. This value may contribute, in part, to the observed As anomaly but does not account for As values of up to 3000 ppm found in selected rock samples (Golding, 1983).

Results for chalcopyrite are approximately the same as above, for Ti and As. Ni levels fall below the detection limit of the electron microprobe and Co levels average about 200 ppm, both considerably lower than for pyrite.

For both sulphides Co/Ni is greater than 1 which is indicative of a hydrothermal source for pyrite and chalcopyrite (Mookherjee & Philip, 1979).

PLATE 4

(a) Adit F, Lady Lehmann Workings
showing contact of the calcite vein
with calcareous siltstones and breccia

(b) Calcite vein, Adit F, containing sulphides,
malachite and limonite staining

(c) Lady Lennon Workings
A typical outcrop of disseminated
mineralisation. Host rocks are
calcarous shales

a

b

c

PLATE 5

(a) Photomicrograph. Reflected light (20x)
Chalcopyrite enclosing inclusion of pyrite.
Rim of chalcopyrite shows alteration to covellite
and chalcocite (top right hand corner).

(b) Photomicrograph.(Reflected Light) (20x)
Chalcopyrite showing alteration to covellite (light blue)
and chalcocite (dull brown).
Calcite gangue (dark brown)

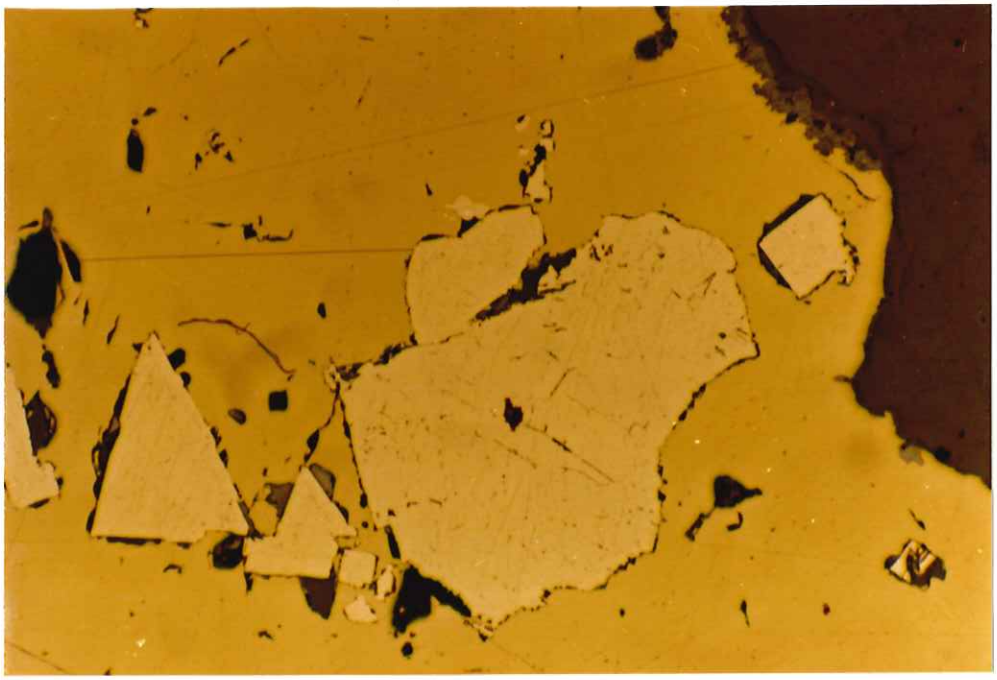

a

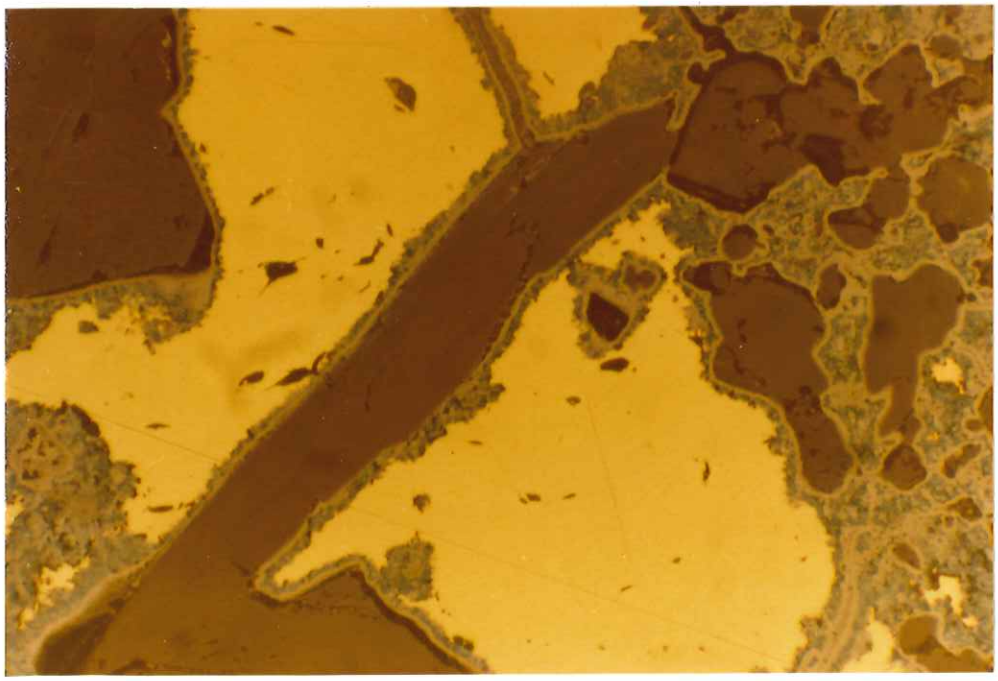

b

PLATE 6

(a) Photomicrograph
Limonite replacement of sulphide showing botryoidal texture
(Transmitted light), (20x)

(b) Photomicrograph of
grain of Electrum (gold) enclosed in gangue groundmass
(Reflected light), (25x)

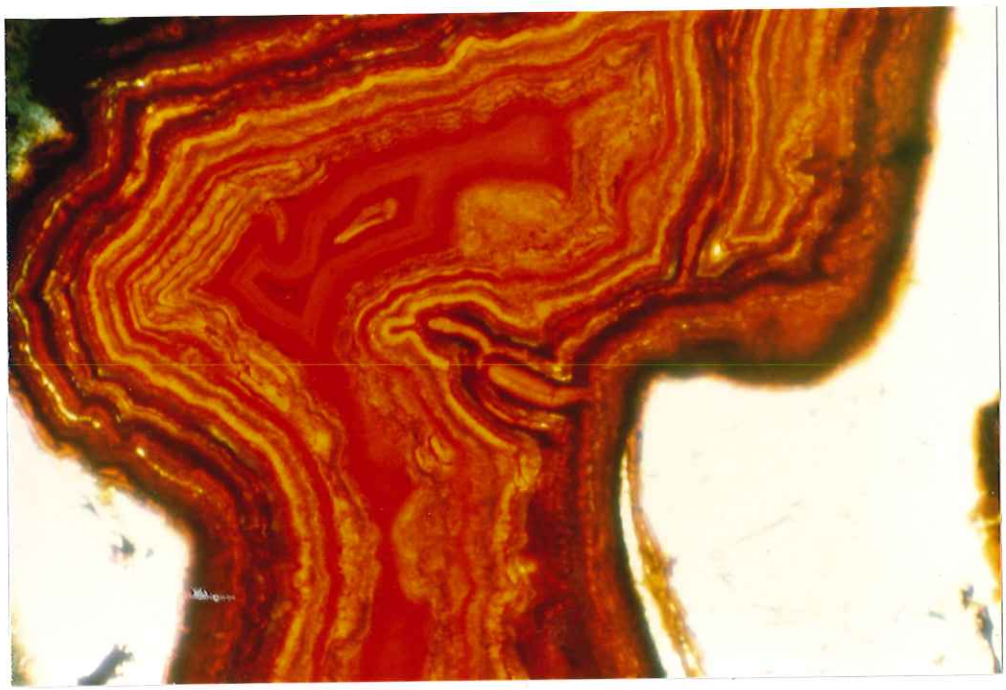

a

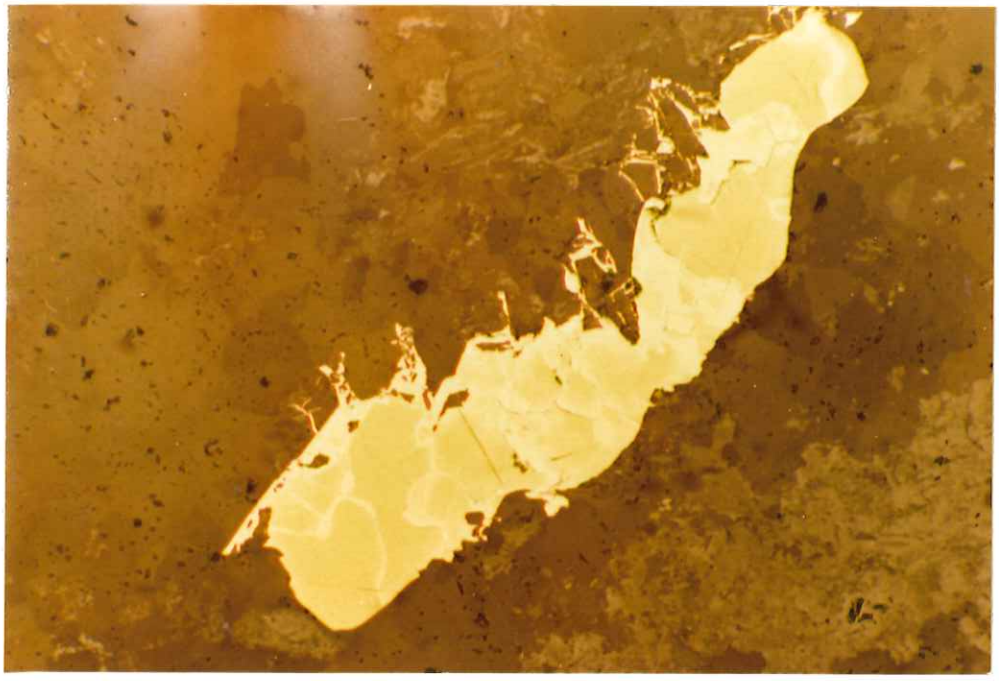

b

4. FLUID INCLUSION STUDY

4.1 Introduction

The use of fluid inclusions to determine the formation temperature of minerals has long been acknowledged and provides one of the most reliable geothermometers available. Basically, a primary inclusion is formed when an imperfection in the crystal face develops during growth and traps a portion of the ore forming fluid, as the crystal grows around this flaw. On cooling the liquid contracts, leaving a near vacuum vapour phase in the inclusion. Heating the inclusion until phase homogenity is accomplished provides a minimum temperature of formation. A pressure correction is then added to the homogenisation temperature to obtain the trapping temperature. Fluid inclusions may also be used to obtain information on the composition of ore forming fluids. A commonly used technique is to determine the freezing point of the fluid in the inclusions and from this to calculate the salinity of the fluid.

All fluid inclusions examined were found in quartz, as the calcite was not translucent enough to permit suitable observation of the inclusions. Samples were taken from the Lady Lehmann and Home Rule Flat workings. Inclusions varied between 10 and 20 um in diameter and generally were irregular in shape. Only inclusions which appeared to be primary and are assumed to form at the same time as the crystal host were investigated.

All inclusions examined were H_2O - brine dominated with relatively low vapour/liquid ratios. The inclusions can be separated into 2 different types (i) Type I which contain H_2O vapour and liquid H_2O and at least one daughter mineral and (ii) Type II which contain H_2O vapour and liquid H_2O. Type I inclusions comprise about 80% of the inclusions examined. The most common daughter mineral is cubic shaped, isotropic, shows low birefringence and occupies between 10 and 20% of the inclusion. This is thought to be halite, although sylvite is another alternative. Other minor daughter minerals show high birefringence and relief and a rhombohedral form.

4.2 Freezing Measurements

Roedder (1962) defined the freezing temperature (final melting temperature) "as that temperature at which the last ice crystal melts in the inclusion, under reversible equilibrium conditions" (ie. increasing temperature). For H_2O- brine systems the freezing temperature is depressed below the freezing temperature for pure H_2O (-0.015°C) and determination of this temperature provides an estimate of the salinity and composition of the fluid within the inclusion. Depending on the temperature recorded, different systems are used to derive the salinity. The H_2O-NaCl system (Figure 6) is generally used if the freezing temperature is between -0.015°C and -21.1°C (the H_2O-NaCl eutectic) and salinity is then expressed in terms of weight % NaCl equivalent. For temperatures less than -21.1°C the $CaCl_2$-H_2O system (Figure 7) may be used and the salinities expressed in terms of weight % $CaCl_2$ equivalent.

The final melting temperatures from which the salinities were obtained are shown graphically in Figure 8 and listed in detail in Appendix 4.

The Type I inclusions would seem to fall into two groups of final melting temperatures. The lower temperature group range between -32.4°C and -22.6°C, which correspond to salinities of 22 to 26 wt % $CaCl_2$ equivalent. The other group have temperatures ranging from -15.4°C to 2.4°C. Since both groups are from the same inclusion type and sample, it is possible that the higher temperatures are due to melting of a NaCl hydrate phase (eg. $NaCl.2H_2O$).

Using the H_2O-NaCl system the higher temperature group correspond to salinities of 24 to 25 wt % NaCl equivalent. However, Sourirajan and Kennedy (1962) state that if daughter minerals are present, then the salinity should be greater than 30 wt % NaCl equivalent.

FIGURE 6 The $NaCl - H_2O$ System

(after Roedder, 1962)

FIGURE 7 The $CaCl_2 - H_2O$ System

(after Ypma, 1979)

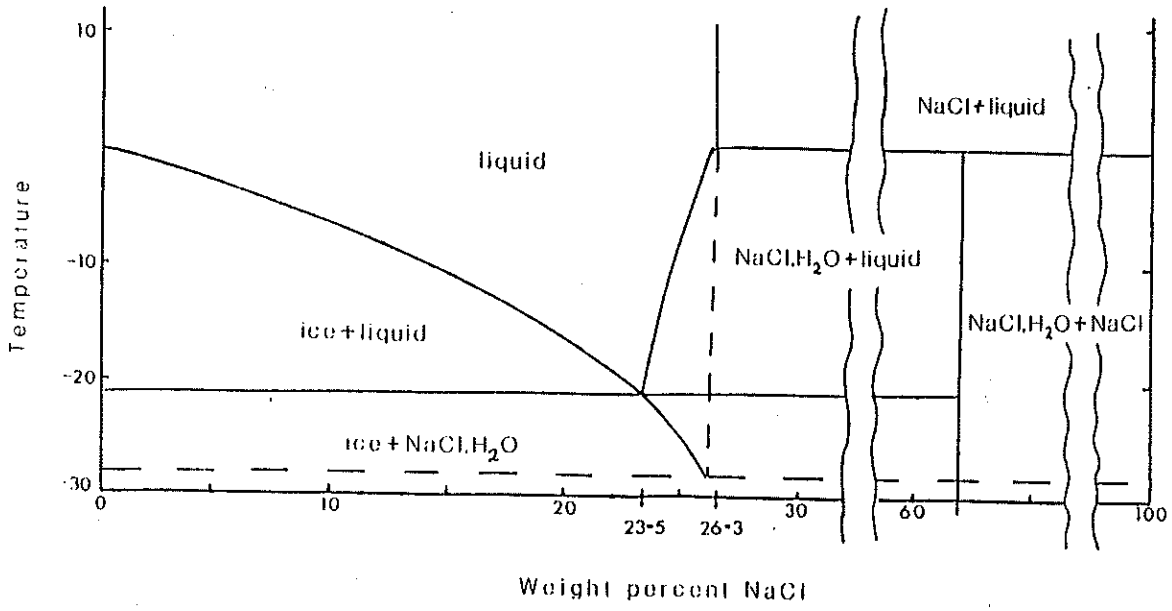

FIGURE 6

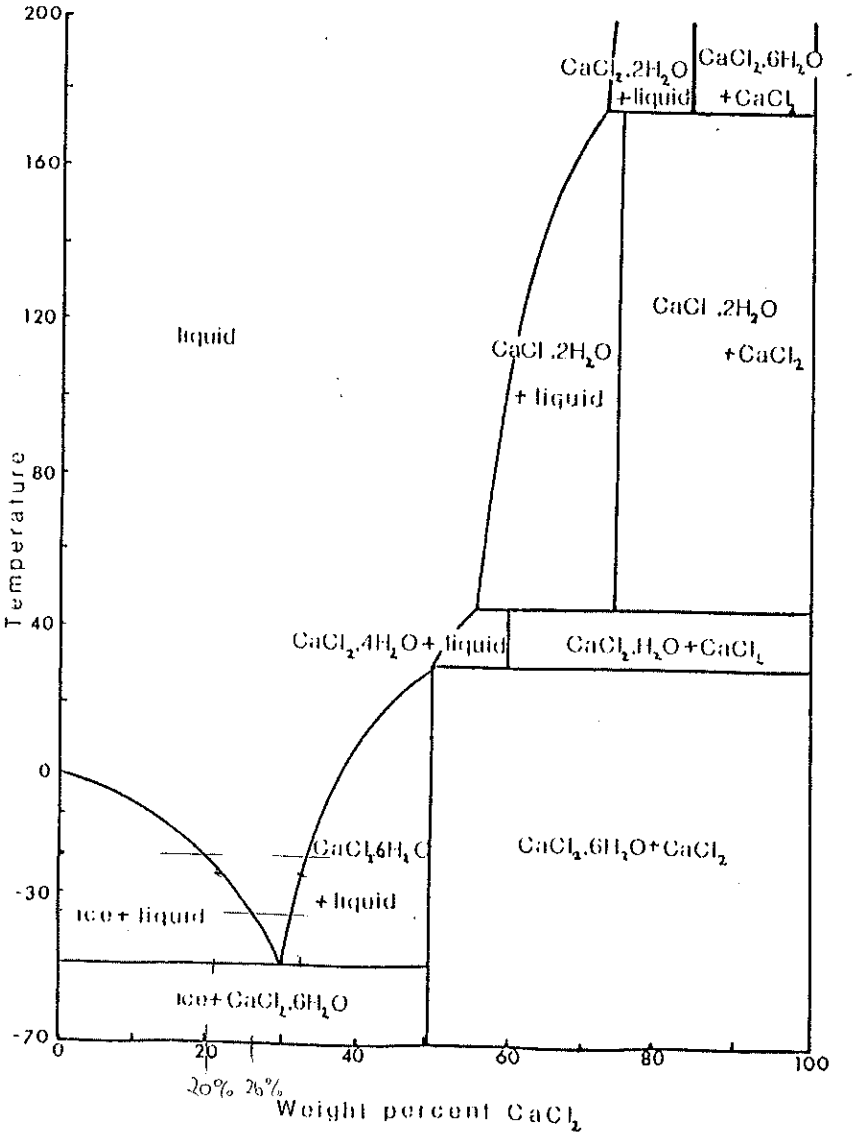

FIGURE 7

Type II inclusions cover a range of values similar to Type I inclusions although they cannot be split into 2 groups (Figure 8). One inclusion shows a positive melting temperature of +1.8°C. This may indicate that the melting phase was NaCl hydrate, existing metastably above its melting point (+0.1°C). This corresponds to a salinity of approximately 26 wt % NaCl equivalent.

The first melting temperatures of Type I and II inclusions show a range of -45.2°C to -19.2°C, and with the exception of three inclusions, all lie below the H_2O-NaCl eutectic (-21.1°C). This implies the presence of $CaCl_2$ and/or $MgCl_2$ (Ypma, 1979). However, electron microprobe studies of some of the inclusions indicate that Na, Cl, Ca and K are present but Mg is not, using the inclusion analysis method outlined by Bone et. al. 1984. This suggests that the fluid compositions could be accommodated in the $CaCl_2$ + NaCl + H_2O system (Figure 9).

4.3 Temperature of Homogenisation

For this study, the homogenisation runs were duplicated on each inclusion. About 10% of the inclusions failed to regain their bubbles immediately on cooling. Because of the general small size and optically poor quality of the inclusions, the temperatures recorded have an uncertainty of $\pm$ 2.0°C, due to visual limitations of the observer.

The homogenisation data are reproduced in Figure 10 in histogram form. Temperatures ranged from 142°C to 176°C with the average temperature being approximately 155°C. On heating of the inclusions, over 80% of daughter minerals remain undissolved, well past the homogenisation temperature. This indicates a low thermal coefficient of stability which is indicative of halite. The pressure correction is considered to be minimal (5°C) as the veins are thought to have formed in open fractures and hydrostatic pressure would dominate (Jouett, 1975).

FIGURE 8 Final Melt Temperatures

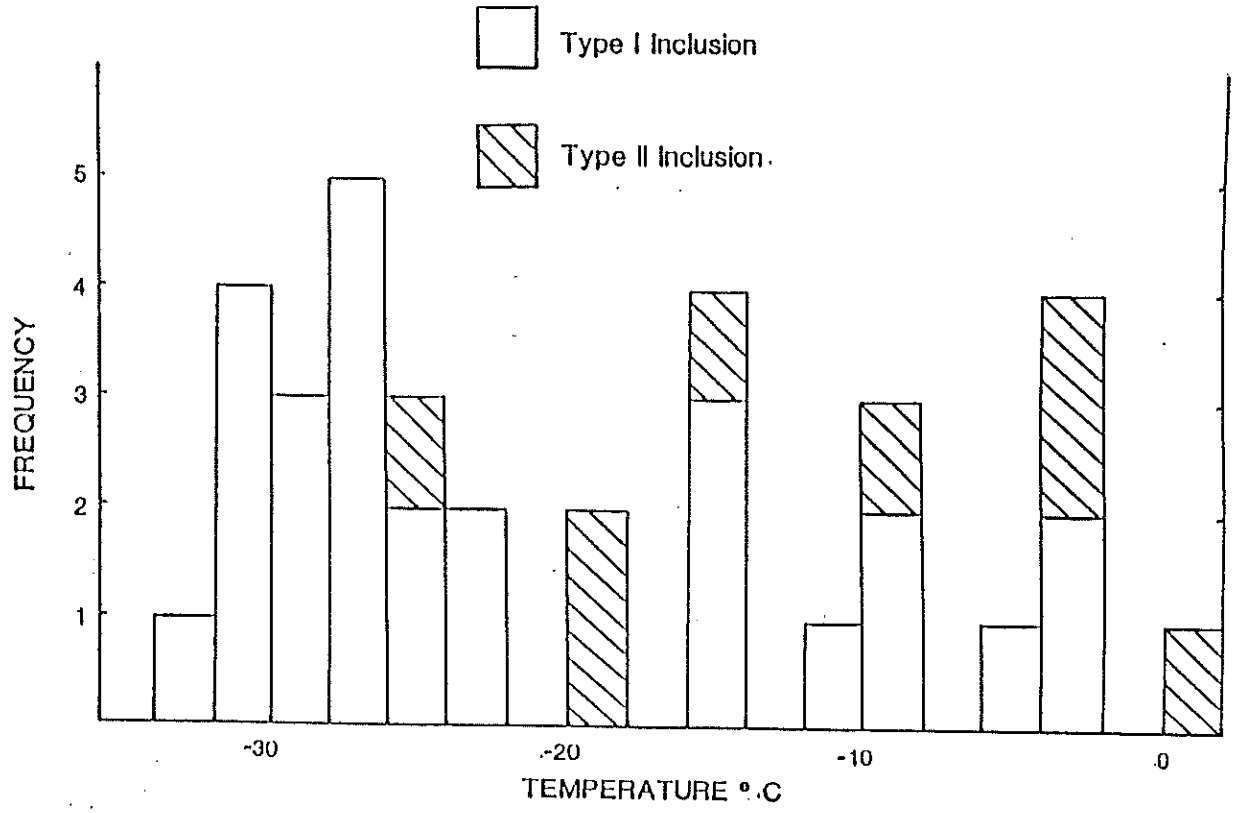

FIGURE 10 Homogenisation Temperatures

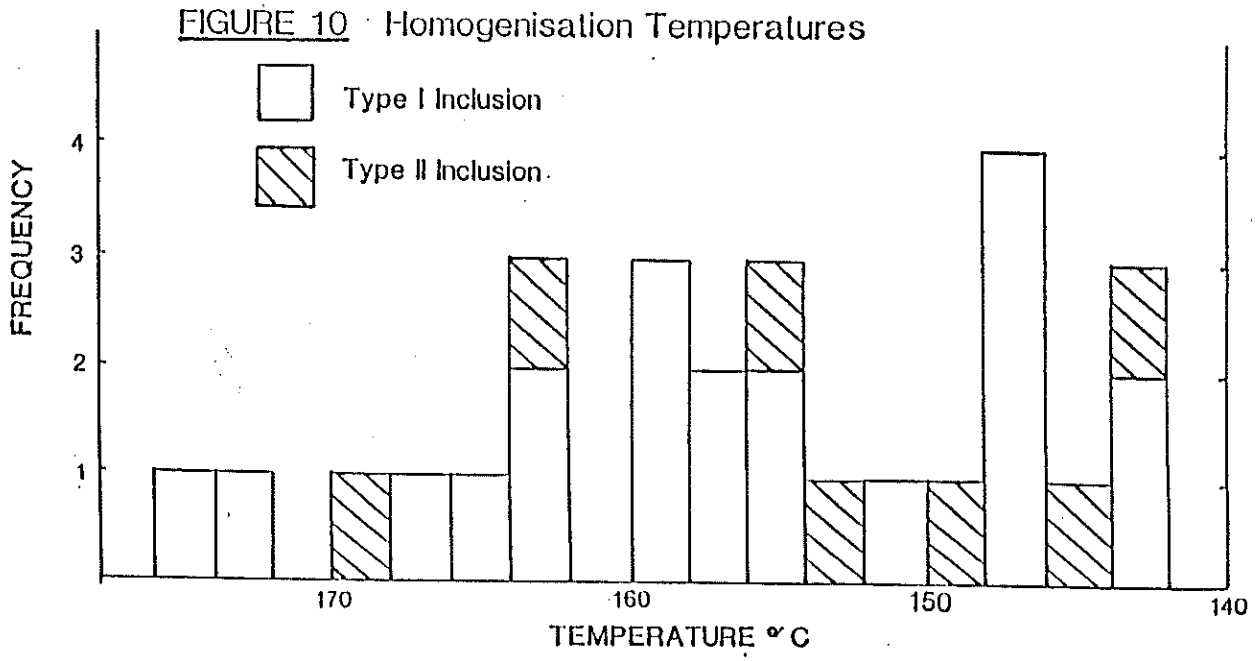

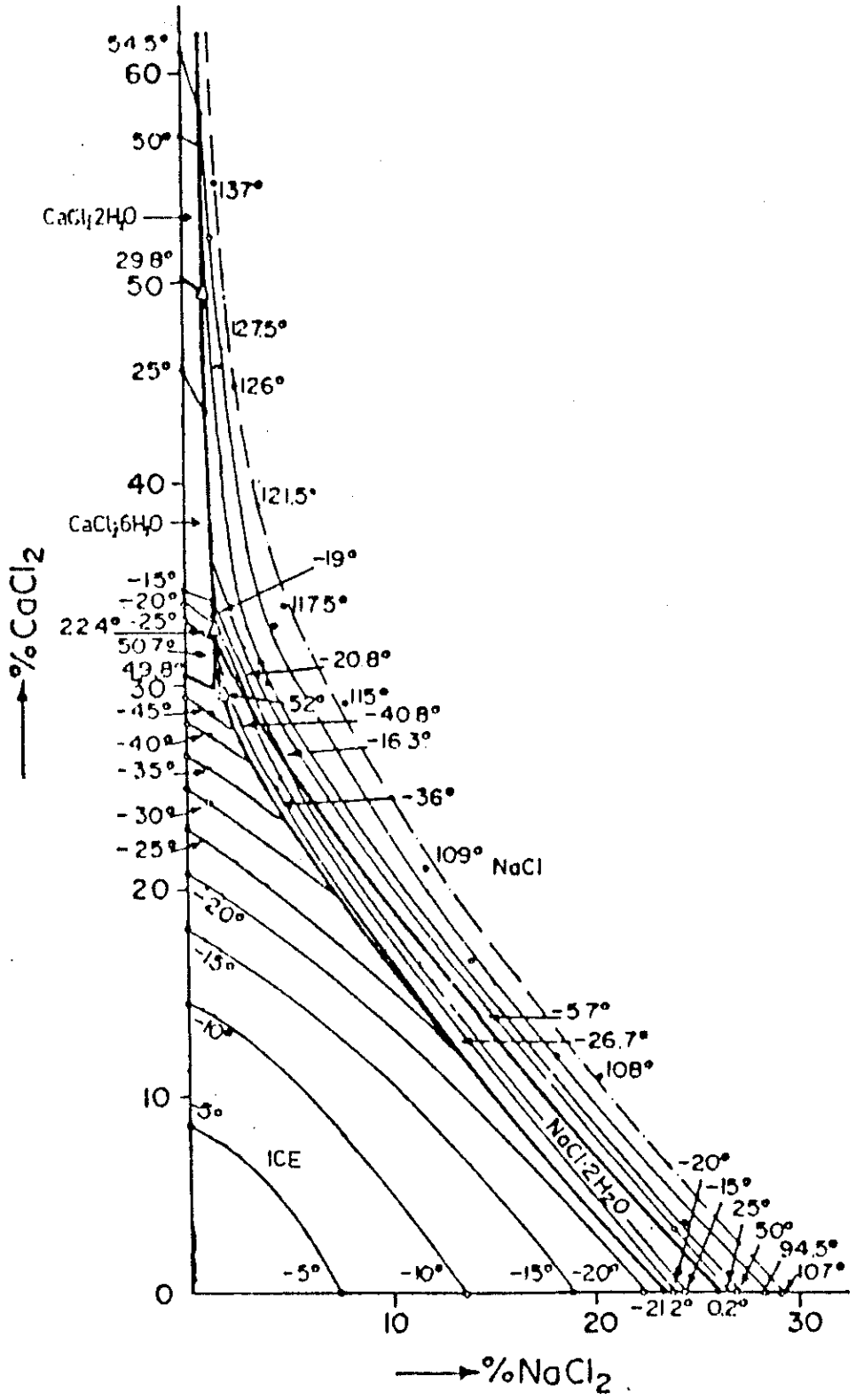

FIGURE 9 $CaCl_2$-NaCl-H_2O System

(after Ypma, 1979)

PLATE 7

(a) Schematic diagram of inclusions examined

(b) Both Type I and Type II inclusions are evident

(c) Typical inclusions contained within quartz samples

(d) Type I inclusion

(e) Regularly shaped Type II inclusion with unusually large daughter mineral and vapour bubble.

(a)

TYPE 1 INCLUSION

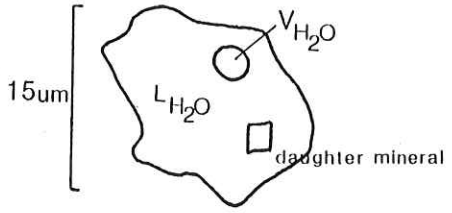

TYPE II INCLUSION

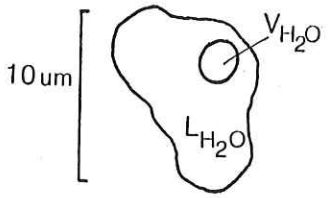

(b)

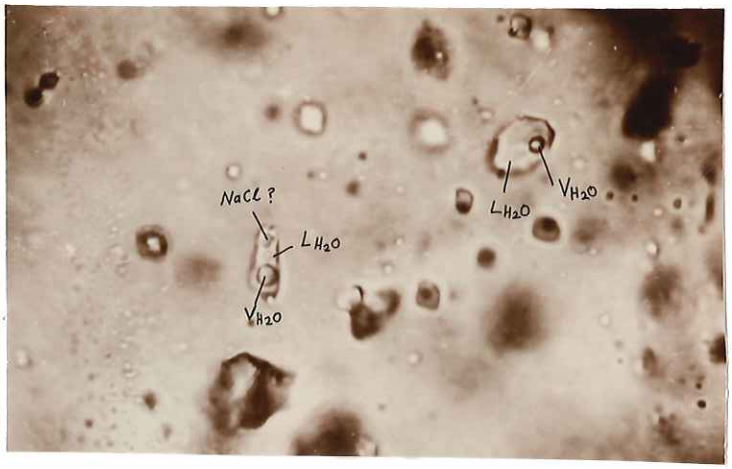

50 μm

(c)

50 μm

(d)

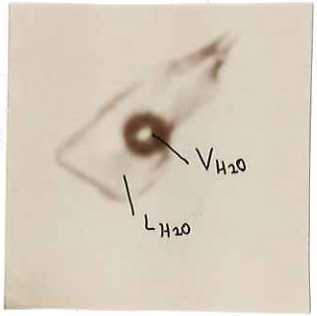

(e)

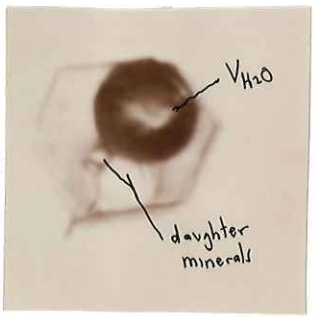

10 μm

5. SULPHUR ISOTOPE STUDIES

5.1 Introduction

Sulphur in hydrothermal ore deposits has originated ultimately from (i) an igneous source or (ii) a sea water source. Sulphur from an igneous source includes sulphur carried in magmatic fluids and sulphur obtained by leaching of sulphur-bearing minerals in igneous rocks. Sulphur in sea water occurs as aqueous sulphates and may be incorporated into sulphide deposits through various paths. Near the earth's surface in-situ reduction of sulphate to H_2S by sulphur reducing bacteria may generate sedimentary sulphides. These may be leached by hydrothermal fluids or they may be replaced by other sulphide minerals when metal bearing brines are encountered. Reduction of aqueous sulphates to aqueous sulphides can take place non-bacterially at elevated temperatures. Therefore sulphate-bearing sea water, sulphate-rich connate or meteoric water bearing sulphate dissolved from evaporites can evolve into sulphide-bearing hydrothermal fluids. Fractionation of sulphur isotopes may occur in a variety of situations in the history of an ore fluid and so the observed $\delta^{34}S$ values of hydrothermal minerals may reflect a complex geochemical history of the sulphur in hydrothermal fluids. Sulphides analysed in the Patawarta Diapir were chalcopyrite and pyrite from the Lady Lehmann and Lady Lennon workings. The results are shown below in Table 3.

TABLE 3 RESULTS OF SULPHUR ISOTOPE MEASUREMENTS

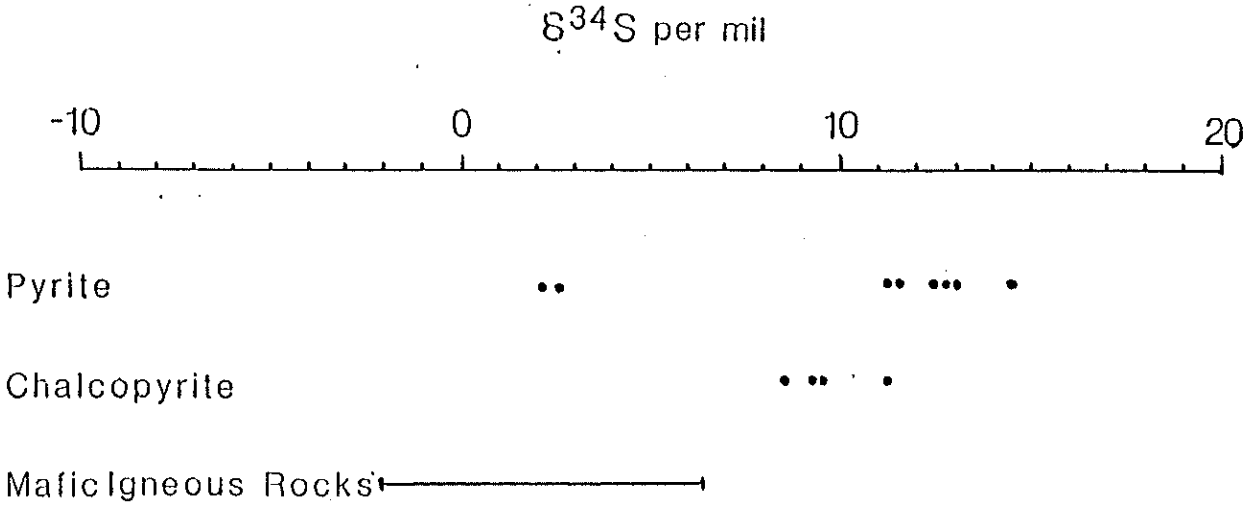

5.2 Geothermometry

Sulphur isotope geothermometry is based on the equilibrium sulphur isotope fractionation between co-existing sulphur-bearing compounds, as the fractionation factor is inversely proportional to the temperature under equilibrium conditions. The sulphur isotope fractionations among sulphur species are given in Figure 13 (Ohmoto & Rye, 1979). The greater the separation of the curves for any two minerals the better the pair will be as an isotopic thermometer.

For application in geothermometry, one requires co-existing sulphides formed at the same time and in isotopic equilibrium and this is often difficult to achieve. For example, relationships between co-existing sulphide minerals in which later minerals were formed by replacement of earlier minerals do not always indicate

(b) $\delta^{34}S_{\Sigma S}$ (the sulphur isotopic composition of the fluid), which is controlled by the source of sulphur

(c) the proportions of oxidised and reduced (ie. H_2S or HS^-) sulphur species in solution.

The origin of sulphur can be discussed only on the basis of the interpreted isotopic composition of the total sulphur in solution ($\delta^{34}S_{\Sigma S}$) Pyrite, for example, which along with chalcopyrite is one of the major sulphides found in the Patawarta Diapir, can obtain values of $\delta^{34}S$ (per mil) similar to the value of $\delta^{34}S_{\Sigma S}$ if:

(i) the sulphur in the fluids is dominated by one species eg. H_2S.

(ii) the relative isotopic enrichment factor between pyrite and the aqueous species is small.

Fluid inclusion studies show that homogenisation termperatures for the veins range from 142°C to 176°C (see figure 10) and for the purposes of this study a temperature of formation of 150°C will be assumed. The hydrothermal solutions are assumed to be slightly acidic or neutral (Anderson, 1973). Figure 11, (Crerar and Barnes, 1976), which shows the predominant regions of H_2S and HS^- and the temperature dependent curve for neutral pH, indicates a neutral pH for H_2S of 5.9 for a temperature of 150°C.

The Fe-S-O stability fields and the sulphur species stability fields are plotted in Figure 12 for 150°C and for ΣS = 0.001 moles/kg H_2O. It can be seen that the pyrite stability field lies mainly in the H_2S dominated sulphur species field for pH values less than 5.9. Thus condition (i) above is fulfilled.

Figure 13 shows that the isotopic enrichment factor between pyrite and H_2S at 150°C is approximately +2 per mil, thus fulfilling condition (ii) above. (for chalcopyrite the corresponding value is -1 per mil).

Therefore the $\delta^{34}S$ values for the sulphide minerals can be assumed to approximate the $\delta^{34}S_{\Sigma S}$ values and so the results can now be interpreted on this basis.

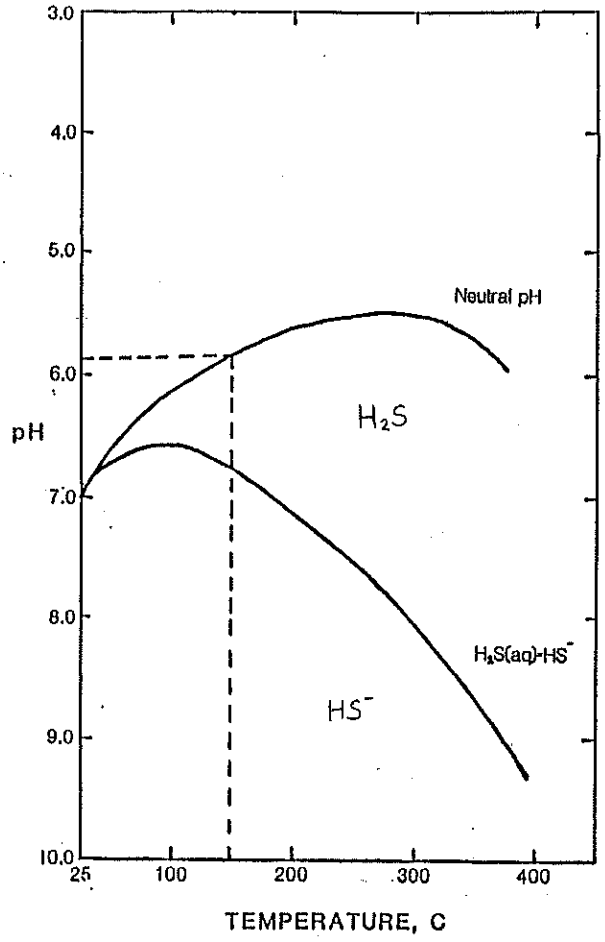

FIGURE 11 Temperature dependant curve for neutral pH & predominance regions for HS^- & H_2S (after Crerar and Barnes (1976))

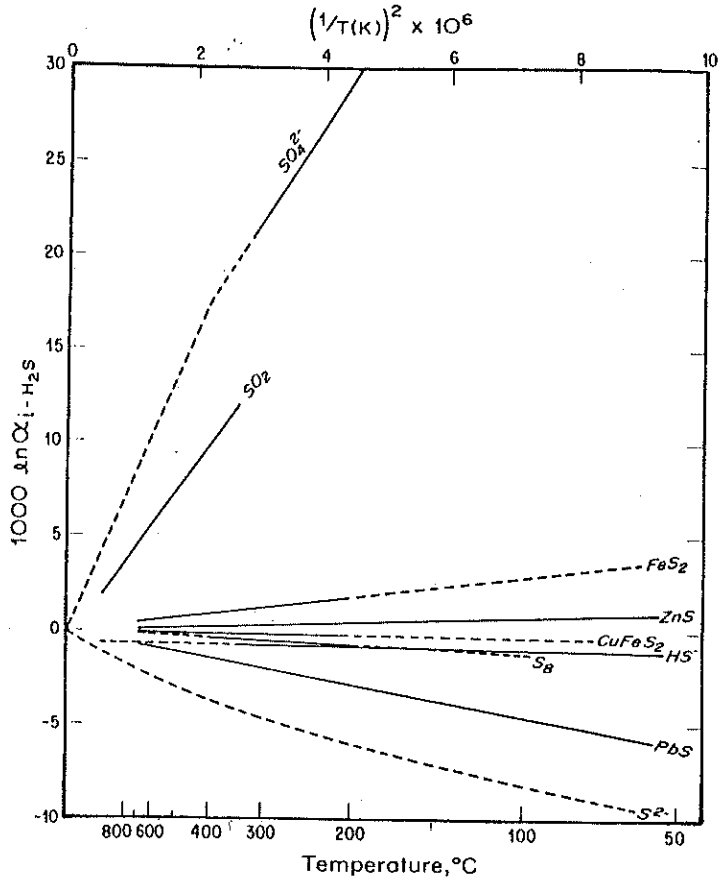

FIGURE 13 Equilibrium Isotopic Fractionation Factors Among Sulfur Compounds Relative To H_2S (after Rye and Ohmoto (1979))

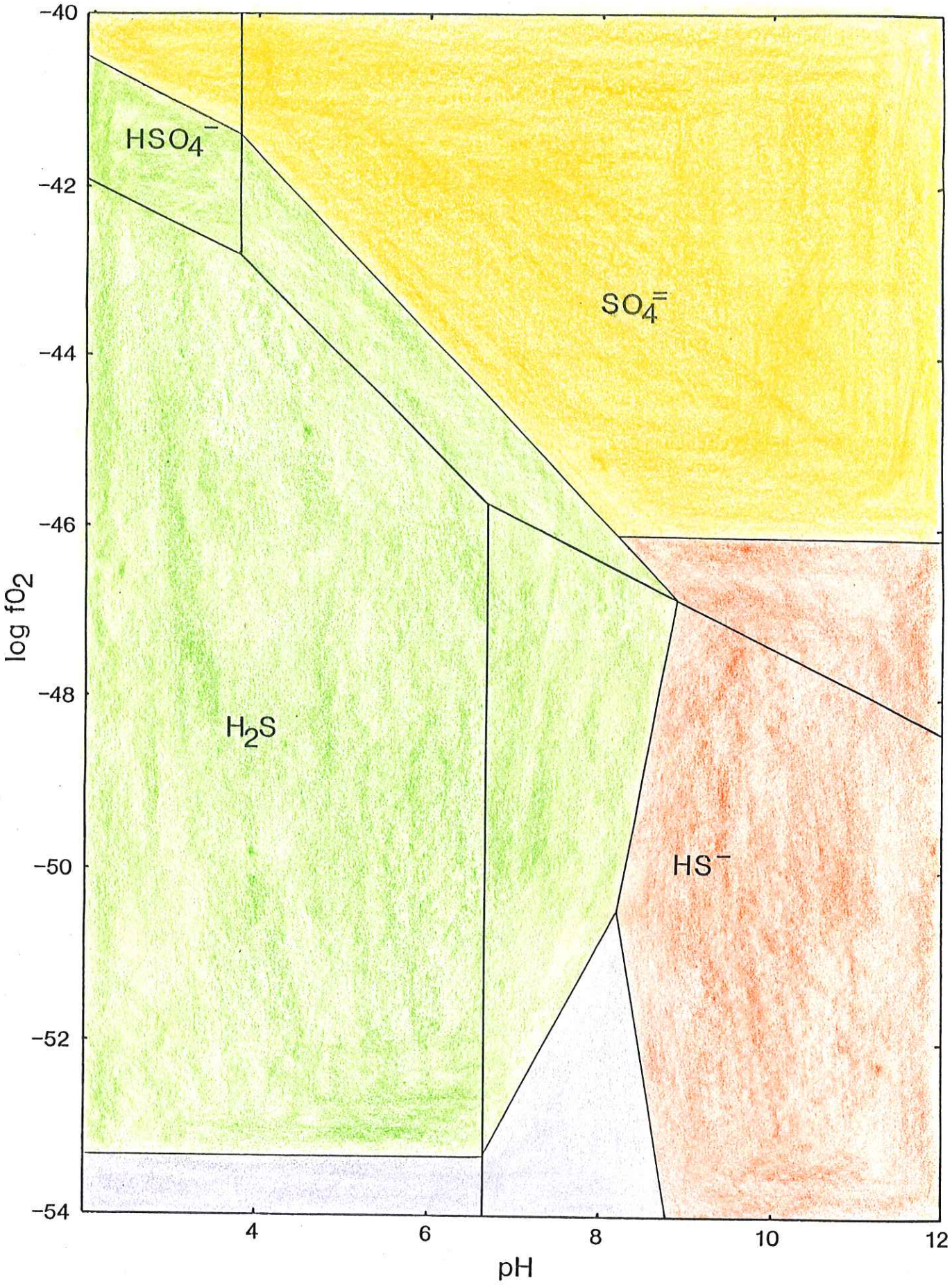

FIGURE 12 Stability fields of Fe-S-O Minerals & sulphur species
($\Sigma S = 0.001$ moles/kg H_2O) ($T°C = 150°$)

FeS_2 FeS Fe_2O_3 Fe_3O_4

——— Sulphur species boundary

The results fall into 2 groups and may indicate a dual source of sulphur in the deposits. The smaller group, consisting of only two pyrite samples, has slightly positive values which fall within the range for mafic igneous rocks. These values may reflect sulphur derived largely from igneous rocks, ie. sulphur released from melts or sulphur leached from sulphides in igneous rocks.

At least the greater contribution of sulphur comes from the second group which have values ranging from 8.5 to 14.4 per mil. This may indicate a source from local country rocks either from sedimentary rocks or evaporites.

Figure 14 (Claypool et. al. 1980) summarizes the relationship between age and sulphur isotopic composition of sea water sulphates. A comparison of $\delta^{34}S$ of evaporites of Precambrian age shows them to be slightly higher that the $\delta^{34}S$ results for this study. This could be due to a sulphur component from a mafic igneous sulphur source which would lower the $\delta^{34}S$ values slightly.

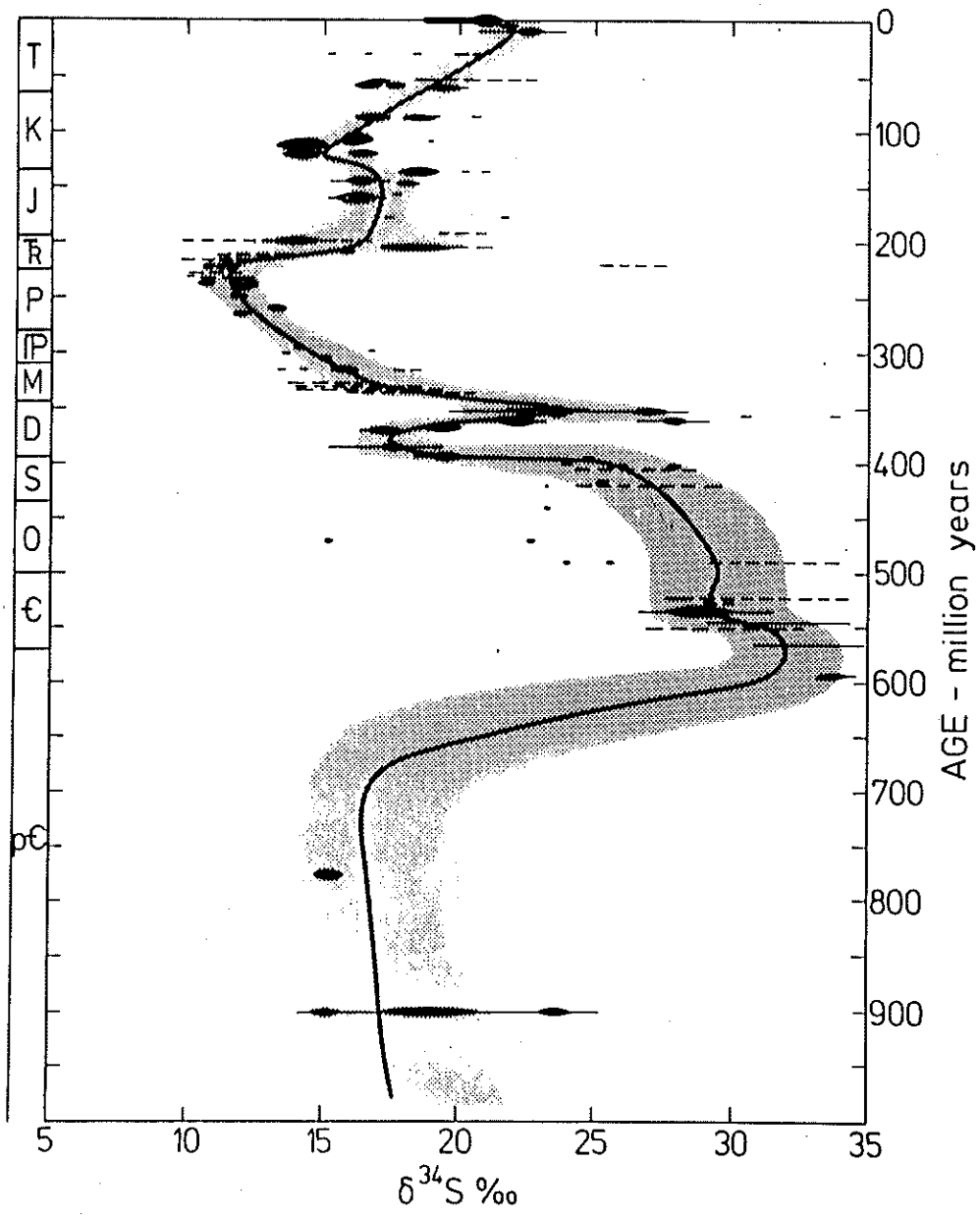

FIGURE 14 Sulphur Isotope Age Curve For Sulphate

(after Claypool et al.(1980))

6. CONDITIONS FOR FORMATION OF THE MINERALISATION

Figure 15 was constructed in an attempt to define the approximate physical and chemical conditions (T, fO_2, pH, $\delta^{34}S_{\Sigma S}$) of the hydrothermal fluids that precipitated mineralisation in the Patawarta Diapir as determined from a study of mineral assemblages and fluid inclusion data. Equilibrium constants for reactions used in the calculation of the figure are listed in Appendix 7. The figure has been constructed for a temperature of 150°C and ΣS = 0.001 moles/kg H_2O. This temperature is based on fluid inclusion measurements of homogenisation temperature and sulphur isotope fractionation between pyrite and chalcopyrite. (see sections 4.3 and 5.3) The ΣS concentration is considered reasonable for these small deposits. Any increase in ΣS will increase the area of pyrite stability field by increasing the fO_2 and pH range for pyrite. Pyrite and chalcopyrite have been precipitated throughout formation of the veins and so fO_2 and pH conditions are assumed to have been restricted to the common area shared by the pyrite and chalcopyrite stability fields. Bornite has not been observed in the mineral assemblages and so the chemical environment is assumed to have always been within the area in which chalcopyrite is the stable Cu-Fe-S species.

The diagram has been contoured for $\delta^{34}S_{py}$ values by assuming a sulphur isotopic composition of the fluid of $\delta^{34}S_{\Sigma S}$ = + 10 per mil. The basis for this assumption is that the mean value of $\delta^{34}S_{py}$ values (excluding the two lowest values) is approximately 12 per mil. Since the fractionation between pyrite and H_2S at 150°C is approximately + 2 per mil (Ohmoto & Rye, 1979),

a contour of $\delta^{34}S_{H_2S}$ = + 10 per mil is equivalent to a contour of $\delta^{34}S_{py}$ = + 12 per mil. Under the fO_2 - pH conditions that existed during formation of the Patawarta mineralisation $\delta^{34}S_{H_2S}$ approximates $\delta^{34}S_{\Sigma S}$, since H_2S would have been the dominant sulphur species.

It should be noted that $\delta^{34}S_i$ (species i) contour values have an uncertainty of $\pm$ 10% due to uncertainies in Δi values, but probably fall within $\pm$ 0.5 log fO_2 units for a given pH (Ohmoto, 1972).

Approximate pH constraints on the mineralising fluid chemistry can be derived from silicate alteration assemblages in the wall rocks of the veins. K-feldspar in the siltstones shows alteration to sericite and using the sericite boundary reaction,

$$3KAlSi_3O_8 + 2H^+ = KAl_2AlSi_3O_{10}(OH)_2 + 2K^+ + 6SiO_2$$

(orthoclase) (sericite)

an upper pH limit can be given, assuming a K^+ concentration. Taking $aK^+ = 0.01$ gives a pH of 7.1 which seems a realistic upper limit for hydrothermal brines. For comparative purposes pH is also derived for an assumed aK^+ of 0.1.

Constraints on the fO_2 of mineralisation can be determined by considering the concentration of Fe in sphalerite. The diagram shows the pyrite field contoured for mole percent FeS in sphalerite. Electron microprobe analyses show that the FeS content of sphalerite in the veins varies between 0.2 and 0.6 mole percent (Appendix 6), indicating log fO_2 conditions of between -48.7 and -49.7.

A lower pH constraint cannot be accurately determined but is unlikely to be less than 4.4 as experimental studies indicate that chloride brines co-existing with muscovite bearing assemblages are weakly acidic (Hemley et al, 1967) and neutral pH at 150°C is about 5.9.

FIGURE 15 Constraints on mineralisation ($T°C = 150°$)

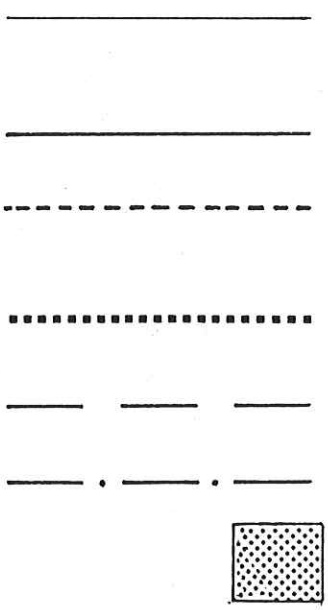

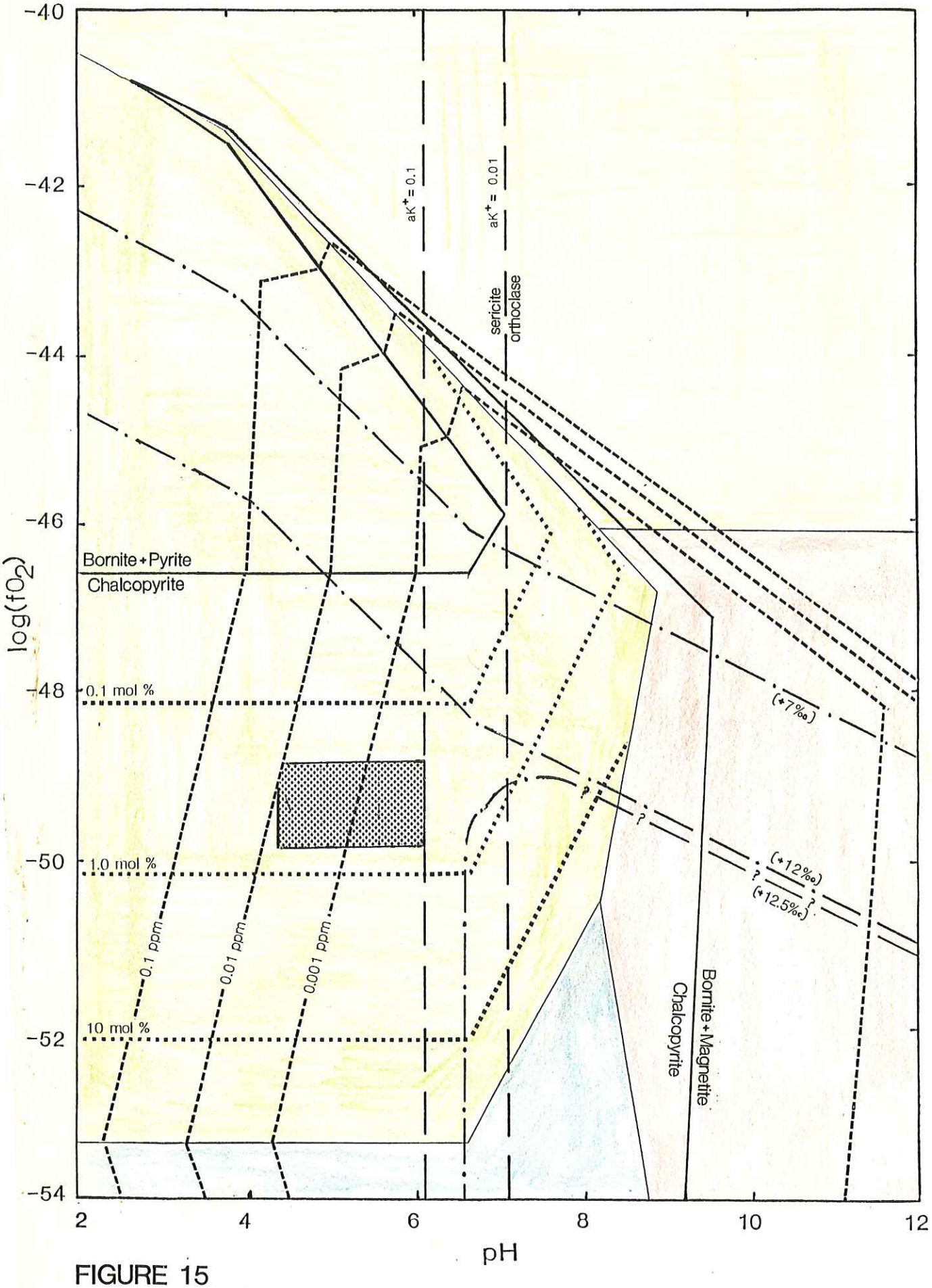
-40
-42
-44
-46
-48
-50
-52
-54
log(fO2)
2
4
6
8
10
12
pH
aK+ = 0.1
aK+ = 0.01
sericite
orthoclase
Bornite + Pyrite
Chalcopyrite
0.1 mol %
1.0 mol %
10 mol %
0.1 ppm
0.01 ppm
0.001 ppm
(+7‰)
(+12‰)
(+12.5‰)
Chalcopyrite
Bornite + Magnetite

FIGURE 15

7. GENESIS OF THE MINERALISED VEINS

In considering the genesis of the vein deposits in the Patawarta Diapir, four aspects have to be considered:

(i) a source for the constituents of the mineralisation must exist, ie. magmatic or sedimentary rocks.

(ii) the dissolution of the mineralising constituents in the brine where the brine may be magmatic water, connate water, etc.

(iii) migration of the metal-bearing fluid.

(iv) selective precipitation of the mineralising constituents in favourable environments.

The source of Cu deposited in the diapir does not seem to pose any problems. Almost all diapirs in the Flinders Ranges show anomalous concentrations of Cu. Many other small deposits occur in Precambrian and Cambrian rocks throughout the Flinders Ranges and Mount Lofty Ranges and large Cu deposits occur at Burra and Kanmantoo. Uneconomic amounts of Cu are known to occur in some Adelaidean System sediments (eg. Bunyeroo Formation) over distances of hundreds of kilometres and small Cu-bearing veins occur locally near many of the major faults. Therefore the whole region is clearly a Cu anomalous province and it is highly likely that the basement rocks, which underlie the Proterozoic sediments in the Adelaide Geosyncline, are enriched in Cu.

Fluid inclusions in minerals in the veins contain greater than 20 wt. % dissolved solids and are rich in Ca, Na, K and Cl ions. In a study of Mississippi Valley type brines which have similar constituents to those described above, Davidson (1968),

suggested that the brines were comparable with "connate waters which have derived the contents of salts by the diagenesis and leaching of evaporitic deposits". This agrees with the interpretation of the sulphur isotope results which indicate a predominant sulphur source from evaporites (section 5.3). In the Adelaide Geosyncline, evaporites are common in the Callanna Beds which represent the earliest Adelaidean sediments. This lithology is interpreted as forming in a sabkha and playa environment (section 2.3.1).

Bush (1970), has discussed the chemical composition of brines from a sabkha environment and comparison of these brines with the composition of fluid inclusions in the veins of the diapir show them to be quite similar. The only major difference is the Mg concentration which falls below the detection limits of the electron microprobe for the diapiric inclusions. The Mg contents of the sabkha brine are considerably higher. Therefore the origin of the vein forming solutions in the Patawarta Diapir could be through the compaction of Callanna Bed sediments. Compaction of sediments and escape of interstitial water start at the time of deposition and continue for millions of years where the initial driving force is lithostatic pressure (White, 1968). Fine grained sediments act as semipermeable membranes allowing selective escape of water and concentration dissolved components in the remaining pore fluids (White, 1968). The brine is later squeezed out of the pores and its reaction with carbonate rocks exchanges Na and Mg for Ca (White, 1968).

It has long been recognised that saline Na-Ca-Cl brines are capable of leaching base metals from the rocks and minerals through which they pass and transport them as chloride complexes over long distances. However, this ability is greatly reduced if sulphur species are present in the brines in any appreciable concentrations.

Over the years, many different mechanisms have been proposed to account for the transportation and precipitation of base metals and sulphur in hydrothemal deposits. These mechanisms can be grouped into three alternative models.

The first, known as a mixing model suggests that reduced sulphur is transported in one solution, base metals are transported in another solution and precipitation takes place where the two solutions mix. Variations on this model suggest that base metals are transported to the site of deposition where they encounter a source of reduced sulphur, such as diagenetic iron sulphides, which cause precipitation.

The second, a sulphate reduction model, suggests that base metals were transported with sulphate in solution and precipitation takes place due to a reaction which causes sulphate to be reduced to sulphide, for example, through the oxidation of organic matter (Barton, 1967).

The third, a reduced sulphur model involves base metals and reduced sulphur (H_2S or HS^-) being transported together in the same solution at low concentrations. The cause of precipitation for this model could be (i) change of pH from acid to neutral (Helgeson, 1970) (ii) cooling or (iii) dilution (Anderson, 1973).

The reduced sulphur model would appear to provide a possible explanation for the Cu mineralisation in the diapir. Cu solubilities have been plotted for a total sulphur content of 0.001 moles/kg H_2O (Figure 16). The 0.001 ppm $\pm$ 0.01 ppm contours intersect the log fO_2 - pH field indicated for mineralisation. Although this value for Cu solubility is low it should be remembered that the Cu content in the veins is quite low and is disseminated. Therefore 0.01 ppm Cu in solution may provide sufficient Cu to generate a deposit of this size.

Dunham (1970) pointed out that one of the conditions necessary for the formation of a high concentration of sulphide is "long continuous flow along restricted paths which may be controlled by stratigraphy or structure". He noted that "if the paths are unrestricted, the mineralisation is likely to be dissipated" such may have been the case for the mineralisation in the Patawarta Diapir. White (1968) also discussed the behaviour of high chloride brines which will dissolve heavy metals and stated that "channels of flow eventually converge upwards towards any through going structures such as faults and fractures".

Many authors have noted that diapiric breccia zones occur in the cores of anticlines and domes which were zones of low pressure during folding. It has been suggested that these become zones of low hydrostatic pressure and this may have played a major role in directing the upward flow of deep formation brines through the rocks. Also, heat from possible post-Willouran igneous activity would have contributed to the increased circulation of deep formation brines through the breccias. Cu would be deposited where the brines encountered an increase in pH or decrease in temperature or underwent dilution.

CONCLUSIONS

1. Primary mineralisation consists of very disseminated chalcopyrite, pyrite, calcite with minor quantities of sphalerite, marcasite and quartz. Secondary alteration products are malachite, limonite, chalcocite and covellite.

2. Fluid inclusion studies indicate:
   (i) Uncorrected temperatures of mineralisaton ranging from 142°C to 176°C with an average of 155°C.
   (ii) Salinities greater than 20 wt % $CaCl_2$ + NaCl equivalent.

3. Sulphur isotope studies indicate:
   (i) Some pyrite-chalcopyrite pairs approached sulphur isotopic equilibrium.
   (ii) A dual source for sulphur is probable with the major component derived from evaporites and a minor component derived from a mafic ingeous source.

4. A homogeneous sulphur source $\delta^{34}S_{\Sigma S} \approx +10$ per mil, together with pH and fO_2 were stable during deposition of sulphides.

5. (i) The mineralising brines formed through compaction of evaporitic sequences of the Callanna Beds of Willouran age.
   (ii) The highly saline brines leached base metals from the basement complex and surrounding country rocks and transportation occurred through the zone of weakness caused by diapiric intrusion.
   (iii) Precipitation occurred in open fractures in blocks in the diapir due to change in pH, change in temperature or dilution.

ACKNOWLEDGEMENTS

I wish to thank my supervisors, Dr. R. Both and Dr. B. Daily for discussion and assistance throughout the year and am greatly indebted to Dr. Both and Dr. J. Walshe (Australian National University), for assistance with thermodynamics.

The logistic support of E.Z. Exploration is greatly appreciated, as is the assistance and advice given by Messrs. B.L. Schmidt and G. Circosta.

I would also like to thank Dr. K. Turnbull for the measurements of sulphur isotopic ratios at the Waite Institute of Agriculture, as well as Mr. E. Bleys for advice on fluid inclusion techniques.

I am indebted to the technical staff of the Geology Department and to Dr. B. Griffin of the Adelaide University Election Optical Centre, for assistance in using the electron microprobe.

Finally, I would like to thank Miss L. Williams for the typing of this thesis.

BIBLIOGRAPHY

ANDERSON, G.M. (1973): The hydrothermal transport and deposition of galena and sphalerite near 100°C. Econ. Geol., v. 68, pp. 480-492.

AUSTIN, J.B. (1863): The Mines of South Australia

BARTON, P.B. (1967): Possible role of organic matter in the precipitation of the Mississippi Valley ores. In Symposium on the genesis of stratiform Pb-Zn-F deposits. Econ. Geol., Mem. 3, pp. 371-377.

BINKS, P.J. (1968): Mineral Exploration of diapirs in the Adelaide Geosyncline. Miner. Resour. Rev., S. Aust., 128, pp. 49-53.

BONE, Y. and GRIFFIN, B.J. (1984): Qualitative analysis of the fluid in fluid inclusions, using the electron microprobe. Geol. Soc. of Abst. No. 12, 7th Aust. Geol. Convention, Sydney 1984.

BROWN, H.Y.L. (1908): Record of the Mines of South Australia (Fourth edition) Government Printer, Adelaide.

BUSH, P.R. (1970): Chloride rich brines from sabkha sediments and their possible role in ore formation. Trans. Inst. Min. Met., v. 79, pp. B137-144.

CALLEN, R.A. (1970): Faulting and other structures on the Arrowie 1:63,360 Geological Sheet with notes on mineral deposits, S. Aust. Dept. Mines unpub. report 70/15.

CLAYPOOL, G.E., HOLSTER, W.T., KAPLAN, I.R., SAKAI, H. AND ZAK, I. (1980): The age curves of sulphur and oxygen isotopes in marine sulphate and their mutual interpretation. Chem. Geol. v.28, pp. 199-260.

COATES, R.P. (1964): The geology and mineralisation of the Blinman Dome Diapir, Rept. Invest. Geol. Surv. S.Aust. 26.

COATES, R.P. (1973): Copley explanatory notes 1:250,000 geological series Sheet SH54-9, International Index Dept. Mines, Geol. Surv. S. Aust.

CRERAR, D.A. and BARNES, H.L. (1976): Ore Solution Chemistry V. Solubilities of Chalcopyrite and chalcocite assemblages in hydrothermal solution at 200° to 350°C. Eco. Geol. v. 71, pp. 772-794.

DAVIDSON, C.F. (1966): Some genetic relationships between ore deposits and evaporites. Trans. Inst. Min. Metal. v. 75 pp. B216-225.

DICKINSON, S.B. (1944): The Lady Lehmann Mine. Dept. Mines S. Aust. Bull. 21, pp. 99-104.

DUNHAM, K.C. (1970): Mineralisation by Deep Formation Waters - a review. Trans. B. Inst. Min. Metal., v. 79, Bull. 765, pp. B127-136.

GOLDING, L.Y. (1983): Report on the Patawarta area, Nuccaleena E.L. E.Z. Exploration unpub. report.

HAAS, J.L. and ROBIE, R.A. (1973): Thermadynamic data for wurstite, magnetite and hematite. (abs). Am. Geophys. Union Trans., v. 54, pp. 438.

HELGESON, H.C. (1969): Thermodynamics of hydrothermal systems at elevated temperatures and pressures. Am. Jour. Sci., v. 267 pp. 729-804.

JOWETT, E.C. (1975): Native of the ore forming fluids of the Polaris lead, zinc deposit, Little Cornwallis Island, N.W.T. from fluid inclusion studies. Bull. Can. Min. Metall. 68, pp. 124-129.

KIJIWARA, Y. and KROUSE, H.R. (1971): Sulphur isotope partitioning in metallic sulphide systems. Can. J. Earth Sci. v. 8, pp. 1397-1408.

MAWSON, D. (1926): The Wooltana Basic Igneous Belt. Trans. Roy. Soc. S.A. v.50. pp. 386-390.

MOOKHERJEE, A. and PHILIP, R. (1979): Distribution of Copper, Cobalt and Nickel in Ores and Host Rocks, Ingladhal, Karnataka, India Mineral. Deposita (Berl.) 14, pp. 33-55.

NAUMOV, G.B., RYZHENKO, B.N. and KHODAKOVSKY, B.L., (1971): Handbook of Thermodynamic data, Moscow, Atomizdat, 323 p (Eng. Rupl. U.S. Geol. Surv.).

OBRIEN, G.D. (1968): Survey of diapirs and diaprism. Am. Ass. Pet. Geol. Mem. 8, pp. 1-9.

OHMOTO, H. (1972): Systematics of sulphur and carbon isotopes in hydrothermal ore deposits. Econ. Geol., v. 67, pp. 551-578.

OHMOTO, H. and RYE, R.O. (1979): Isotopes of Sulphur and Carbon. In Barnes, H.L. (Ed). Geochemistry of Hydrothermal Ore Deposits. (1979), pp. 509-567.

PRIESS, W.V. (1980): Stratigraphy and tectonics of the Worumba Anticline. S.A. Dept. Mines and Energy report 81/82, (unpub.).

READ, R. (1971): Geological report on the Patawarta Diapir. Part SML 557, North Flinders Mines Limited, S.A. Dept. Mines and Energy report 1638, (unpub.).

ROEDDER, E.: (1962): Studies of fluid inclusions, I. Low temperative application of a dual purpose freexing and heating stage. Econ. Geol. v. 57, pp. 1045-1061.

ROSE, A.W., HAWKES, H.E. and WEBB, J.S. (1979): Geochemistry in Mineral Exploration, 2nd edition, Academic Press.

ROWLANDS, N.J., BLIGHT, P.G., JARVIS, D.M. and von der BORCH, C.C. (1980): Sabhka and playa environments in late Proterozoic grabens, Willouran Ranges, South Australia. Journ. Geol. Soc. Aust. v. 27, pp. 55-68.

SCHNEEBERG, E.P. (1973): Sulphur fugacity measurments with the electrochemical cell Ag/AgI, Ag_{2+} X S, fS_2. Econ. Geol. v. 68, pp. 507-517.

SHACKLETON, W.G. (1968):Lady Lehmann Mine, SML 206/1 Minoil Services for Admin. Exploration, S.A. Dept. Mines and Energy report 1013, (unpub.).

SHADE, J.W. (1974): Hydrolosis reactions in the SiO_2 - excess portion of the system K_2O - Al_2O_3 - SiO_2 - H_2O in chloride fluids at magmatic conditions. Econ. Geol. v. 69, pp. 218-228.

SOURIRAJAN, S. and KENNEDY, G.C. (1962): The system H_2O - NaCl at elevated temperatures and pressures Am. J. Sci. 263, pp. 1055-1074.

SPRY, A.H. (1952): Basic Igneous Rocks of the Worumba Region, South Australia., Trans. Roy. Geol. Soc. S.A., v. 75 Sept.

WALSH, J.L. and SOLOMON, M. (1981): An investigation into the environment of formation of the volcanic-hosted Mt. Lyell Copper Deposits., Econ. Geol v.76 pp. 246-284.

WHITE, D.E. (1968): Environments of generation of some base-metal ore deposits. Econ. Geol. v. 63, pp. 301-335.

YPMA, P.J.M. (1979): Water-soluable - CO_2 systems. In: Workshop Manual on Fluid Inclusions. La Trobe University, Melbourne, Melbourne, Australia.

APPENDIX 1

SELECTED ROCK DESCRIPTIONS

Sample 831-150 Diapiric carbonate breccia

Hand Specimen : brown-pale yellow weathered feldspathic dolomitic breccia

Micro Description:		
	Dolomite	60%
	Quartz	10%
	Feldspar	15%
	Calcite	5%
	Talc	3%
	Hematite	5%
	Limonite	2%

The rock is an obvious breccia with fragments of rock up to 2 cm across, making up to 60% of the sample with the carbonate matrix enclosing the fragments. Feldspar includes both microcline and plagioclase, occurring as anhedral grains.
Quartz occurs as anhedral interlocking grains. Limonite is associated with dolomite in fractures and has stained the rock.

Sample 831-146 Rim Dolomite

Hand Specimen : buff coloured massive rock containing numerous clasts

Micro Description: (Matrix)		
	Dolomite	95%
	Quartz	1%
	Ferruginous material	4%

The bulk of the rock is made up of Callanna Bed clasts. The matrix dolomite forms a granular interlocked mosaic with variations in grain size in different parts of the slide. Grains vary up to 0.05 mm in size. Quartz is present as subhedral grains up to 0.3 mm in size.

Sample 831-55 Diapiric Dolomite

Hand Specimen : light brown fine to medium grained carbonate with minor quartz

Micro Description: (Matrix)	Dolomite	90%
	Quartz	8%
	Limonite	2%

The rock is composed of interlocking medium grained carbonate and quartz, clouded by limonite staining. Grains of dolomite are anhedral to polygonal interlocking crystals up to 0.3 mm in size. Quartz occurs on scattered anhedral grains. One grain of subhedral pyrite was noted.

Sample 831-01 Altered Dolerite

Hand Specimen : dark green fine grained altered rock

Micro Description:	Epidote	20%
	Labradorite	10%
	Albite	35%
	Chlorite	5%
	Calcite	15%
	Pyroxene	10%
	Actinolite	5%
	Riebeckite	1%
	Opaques	4%

The rock is a medium grained saussuratised dolerite with euhedral laths of labradorite set in fine grained alteration minerals. Pyroxene occurs as euhedral relic fragments with a pink colouration suggesting titaniferous augite. Chlorite occurs as fine grained fibrous clusters. Fine grained actinolite appears to be replacing pyroxene. Epidote shows yellow pleochroism and occurs as clusters replacing pyroxene. 3 grains of riebeckite were noted.

Mn?

Sample 831-75 Siliceous Mg-Fe rich rock

Hand Specimen : brown siliceous diapiric rock

Micro Description:		
	Quartz	90%
	Limonite	10%

A medium to fine grained rock with anhedral interlocking quartz. Limonite occurs around boundaries of quartz. Minute carbonate blebs within the quartz grains indicate a former abundance of carbonate which may have been leached.

Sample 831-43 Green-brown calcareous siltstone

Hand Specimen : Fine grained green-brown calcareous siltstone

Micro Description:		
	Quartz	30%
	Feldspar	40%
	Calcite	15%
	Opaques	15%

The rock consists of silt-sized quartz and feldspar grains with medium grained calcite grains. The quartz and feldspar grains are subangular to subrounded and appear to be detrital. Feldspar is predominately orthoclose with minor plagioclase. Opaques occur in bands as anhedral detrital grains.

Sample 831-44 Altered Basalt

Hand Specimen : Brecciated dark green medium grained basalt

Micro Description:		
	Plagioclase	10%
	Calcite	10%
	Albite	30%
	Chlorite	5%
	Actinolite	20%
	Hematite	15%
	Epidote	10%

Laths of plagioclase (labradorite) show alteration to albite which is associated with epidote. Epidote occurs as clusters probably replacing pyroxene (?). Chlorite occurs as a fine fibrous form, occasionally intergrown with epidote. Hematite is disseminated and fine grained.

Sample 831-27 Heavy mineral laminated sandstone

Hand Specimen : Heavy mineral laminated sandstone, thinly bedded.

Micro Description:		
	Quartz	80%
	Feldspar	10%
	Hematite	5%
	Carbonate	1%
	Mica	5%

Quartz occurs as poorly sorted fine grains containing overgrowths. Feldspar is thought to be detrital microcline. Hematite occurs as detrital grains and occurs in bands.

Sample 831-150 Hanging Wall Siltstone, Adit F, Lady Lehmann Workings

Hand Specimen :Green, brown siltstone, thinly bedded, with malachite staining

Micro Description:		
	Quartz	10%
	Feldspar	35%
	Sericite	20%
	Limonite	2%
	Pyrite	3%
	Malachite	10%
	Chlorite	3%
	Muscovite	2%

The sample consists of fine - medium grained detrital quartz and feldspar grains cemented by a fine grained phyllosilicate matrix. Quartz and feldspar grains are angular to subrounded. Many orthoclase grains show alteration to sericite, which comproses most of the phyllosilicate matrix. Trace muscovite and chlorite grains are randomly distributed and appear to be detrital. Pyrite grains are disseminated. Malachite forms fine acicular crystals and infills interstices between limonite and quartz and feldspar fragments. Limonite appears to have replaced some of the pyrite grains with a botryoidal form.

Sample 831-143 Vein material, Adit F, Lady Lehmann Workings

Hand Specimen : Massive calcite with disseminated sulphides

Micro Description:	Calcite	75%
	Quartz	10%
	Feldspar	5%
	Sulphides	10%

The vein gangue is made up of both coarse and fine grained fibrous calcite. Subanhedral quartz grains occur in clusters and are medium grained. Occasional albite grains occur in association with quartz. The major sulphides are pyrite and chalcopyrite with grains ranging up to 5 mm in diameter. Pyrite shows an octahedral form.

Chalcopyrite typically comprises 60% of the total sulphides present. Small grains of sphalerite and marcasite are found in association with the major sulphides. Chalcopyrite contains inclusions of pyrite which is not a replacement feature and inclusions of calcite occur in both chalcopyrite and pyrite. Covellite and chalcocite occur as a compact mass of uniform polygonal grains occurring around the rims of the primary sulphides.

Sample 831-145 As above

Hand Specimen : As above

Micro Description:

This rock is very similar to 831-143, except that secondary alteration effects are far more noticeable. Limonite has replaced most of the sulphide grains and shows a botryoidal texture. Malachite forms fine crystals along the boundaries of the altered sulphides.

Sample 831-92 Siderite vein, Lady Lennon Workings

Hand Specimen : Light brown coarse siderite vein with abundant malachite staining and minor sulphides.

Micro Description:

Siderite	65%
Calcite	5%
Quartz	10%
Sulphides	5%
Malachite	10%
Limonite	5%

Coarse grained siderite containing minor quartz and calcite forms the gangue. Medium anhedral grains of chalcopyrite appear disseminated throughout the gangue. Minor anhedral disseminated grains of pyrite occur and pyrite is also present as inclusions within chalcopyrite. Limonite has replaced most of the sulphides and malachite occurs around the rims of the limonite as fine crystals.

Sample 831-85 Calcite -hematite vein, Mosleys Workings

Hand Specimen : Calcite material containing abundant hematite and blebs of malachite.

Micro Description:		
	Calcite	60%
	Hematite	20%
	Malachite	10%
	Sulphides	5%
	Quartz	5%

Coarse grained calcite and disseminated hematite from the matrix in which very minor pyrite and chalcopyrite are contained. Limonite replacement is evident and malachite is abundant through the slide.

Sample 831-124 Calcite vein, Home Rule Flat Workings

Hand Specimen : Ferruginous coarsely crystalline calcite with malachite staining.

Micro Description:		
	Calcite	70%
	Malachite	10%
	Sulphides	1%
	Quartz	2%
	Feldspar	5%
	Limonite	12%

Sample consists essentially of large calcite crystals up to several mm in size intergrown with plagioclase and very minor quartz. Semi opaque limonite is present throughout the slide and has replaced sulphides. Much of the calcite exhibits a colloform texture. Malachite is disseminated throughout the slide. One anhedral grain of electrum is surrounded by calcite.

APPENDIX 2

SELECTED ROCK ANALYSIS

Sample	831-01	Dolerite
	831-44	Basalt (non amygdaloidal)
	831-19	Heavy mineral laminated sandstone
	831-35	Black shale
	831-139	Black limestone
	831-62	Green calcareous siltstone
	831-76	Siliceous Mg-rich rock, near Mt. Rugged Workings
	831-39	Calcite vein, Mount Rugged
	831-59	Siderite vein, Mosleys
	831-83	Diapiric dolomite with malachite Staining
	831-133	Pyritic black shale, Adit. F.
	831-131	Footwall breccia, Adit. F.
	831-61	Typical carbonate breccia
	831-132	Hanging wall siltstone with malachite staining, Adit. F.
	831-125	Calcite vein, Adit. F.
	831-143	Vein material, Adit F.
	831-92	Siderite vein with malachite staining, Lady Lehmann Workings
	831-85	Calcite vein with Lemalite and malachite, Mosleys Workings
	831-124	Calcite vein with malachite staining, Home Rule, Flat.

APPENDIX 2 (continued)

Table A - Major Elements

Sample / Major Elements	01	44	19	35	139	62	76	39
SiO_2	49.17	50.25	64.60	57.31	27.52	57.62	76.92	27.03
Al_2O_3	14.53	15.50	10.59	16.56	6.87	13.44	5.43	0.36
Fe_2O_3	15.19	12.24	3.70	8.21	4.54	5.39	12.06	1.93
MnO	0.12	0.16	0.09	0.05	0.30	0.08	0.08	0.23
MgO	7.59	6.08	0.80	7.07	1.88	5.39	0.62	1.13
CaO	7.31	9.37	12.66	1.73	55.69	6.27	0.16	69.04
Na_2O	3.28	3.42	5.41	3.25	0.58	7.20	0.06	0.09
K_2O	0.70	1.15	0.08	4.48	1.29	2.43	1.84	0.05
TiO_2	1.84	1.92	1.30	0.91	0.52	1.43	0.32	0.02
P_2O_5	0.16	0.19	0.11	0.16	0.12	0.21	0.22	0.00
TOTAL	99.88	100.25	99.34	99.84	99.31	98.47	96.69	99.87

APPENDIX 2 (continued)

Table A - Major Elements

Sample / Major Elements (wt%)	59	83	131	131	61	132	125
SiO_2	1.06	46.18	57.13	56.67	47.18	54.62	0.21
Al_2O_3	0.13	12.85	16.56	14.08	12.86	15.46	0.13
Fe_2O_3	87.59	4.67	8.21	6.27	6.32	6.49	2.51
MnO	0.14	0.32	0.05	0.13	0.28	0.08	0.35
MgO	0.53	13.29	7.07	8.07	8.42	5.38	1.09
CaO	9.68	14.71	1.73	9.51	19.71	8.17	92.57
Na_2O	0.16	0.08	3.25	0.96	3.06	5.38	0.00
K_2O	0.01	7.32	4.48	3.38	4.27	2.87	0.01
TiO_2	0.06	0.64	0.91	0.75	0.41	1.00	0.00
P_2O_5	0.05	0.14	0.16	0.13	0.11	0.15	0.00
TOTAL	99.43	100.28	99.71	99.95	99.47	99.58	96.72

APPENDIX 2 (continued)

Table B - Trace Elements

Trace Elements (ppm) Sample	Cu	Pb	Zn	Ni	Co	As
831-01	0.007	0.0	0.82	150	0.0	0.0
44	2.0	0.0	0.79	62	0.0	0.0
19	0.006	0.0	0.0	0.0	0.0	0.0
35	0.0	0.0	0.0	0.0	0.0	0.0
139	1.2	3.52	95.0	52	10	0.0
62	0.0	0.0	0.0	0.0	0.0	0.0
76	1650	16	11	1.2%	-	27
39	67	18	250	14	57	200
59	9400	26	44	127	10	440
83	1870	0.0	11.1	0.0	0.0	0.0
133	1.2%	140	852	716	550	316
131	9400	10	37	451	21	24
61	0.07	0.0	0.0	0.0	0.0	0.0
132	1.4%	150	870	620	1075	2900
125	1.7%	47	450	150	58	1700
143	2.2%	85	360	124	62	260
92	470	46	152	75	42	850
85	4.4%	0.0	5	0.0	0.0	0.0
124	2.7%	270	860	540	320	440

APPENDIX 3

TRACE ELEMENTS IN SULPHIDES (ppm) wt%?

Pyrite:	Co	Ni	Ti	As	Co/Ni
Sample No : 831-136L	1.0500	0.0033	0.0020	0.0192	318.18
"	0.9197	0.0031	0.0023	0.0345	296.8
"	0.9527	0.0018	0.0000	0.0192	529.3
"	1.0384	0.0023	0.0092	0.0299	451.4
831-136L	0.8752	0.0024	1.2392	0.0166	364.66
"	1.4697	0.0039	0.000	0.0413	376.8
"	0.0518	0.0097	0.0075	0.0273	5.3
831-144L	0.0077	0.0048	0.0143	0.0705	1.61

Chalcopyrite:	Co	Ni	Ti	As	Co/Ni
831-144L	0.0274	0.000	0.0048	0.0310	-
" "	0.0296	0.000	0.0022	0.0338	-
831-136L	0.0341	0.000	0.0073	0.0295	-
"	0.0242	0.000	0.0059	0.0251	-
831-135L	0.0322	0.000	0.0047	0.0297	-

APPENDIX 4

Fluid Inclusion Data Obtained From Patawarta Veins

Inclusion Type	First Melt °C	Final Melt °C	Homogenisation Temperature °C
I	-	-32.4	156.3
"		-30.6	142.0
"	-43.2	-29.7	-
"	-	-28.4	-
"	-	-22.6	143.4
"	-	-23.4	163.7
"	-	-24.5	154.3
"	-40.9	-24.1	-
"	-45.2	-26.9	147.8
"	-41.4	-30.1	146.5
"	-	-29.7	-
"	-44.2	-32.1	158.4
"	-	-27.6	-
"	-36.4	-	162.7
"	-	-26.4	146.4
"	-39.7	-26.7	-
"	-	-31.3	175.9
"	-38.4	-27.0	168.7
"	-28.7	-8.7	-
"	-24.2	-4.2	159.4
"	-	-3.1	-
"	-	-2.4	147.6
"	-31.2	-14.7	-
"	-	-15.4	171.4
"	-	10.2	158.7
"	-	-9.5	-
"	-	-	163.2
"	-	-	174.4
"	-	-	165.4
"	-	-	156.7
"	-	-	154.3
"	-	-	162.4
II	-	+1.8	154.7
"	-	-2.2	-
"	-	-19.2	144.2
"	-	-18.4	151.2
"	20.4	-2.8	-
"	20.7	-10.7	-
"	-	-19.3	154.9
"	-	-15.7	-
"	-	-19.7	157.3
"	-	-24.6	-
"			149.2
"			144.2

APPENDIX 5

RESULTS OF THE SULPHUR ISOTOPE STUDY

SAMPLE	$S^{34}S_{Chalcopyrite}$ (‰)	$S^{34}S_{Pyrite}$ (‰)
LADY LEHMANN MINE:		
831-136*	+10.4	+12.6
831-144*	+ 8.5	+11.4
831-139	+ 8.6	+ 2.1
831-143	-	+14.4
831-145	-	+12.4
831-137	+ 9.3	+11.2
831-138	-	+ 2.5
LADY LENNON MINE:		
831-129	+ 8.6	+12.8

* - coexisting sulphide pairs

Sample was ?

APPENDIX 6

Electron Microprobe Analysis Of Concentration of Fe In Sphalerite

	Element	wt %	atm fraction
	Fe	0.14	0.001
1.	Zn	66.96	0.497
	S	33.10	0.501
	Total	100.21	1.000
	Fe	0.27	0.003
2.	Zn	66.85	2.496
	S	33.10	0.501
	Total	100.25	1.000
	Fe	0.23	0.002
3.	Zn	67.36	0.498
	S	33.21	0.500
	Total	100.80	1.000
	Fe	0.21	0.002
4.	Zn	66.89	0.497
	S	33.03	0.501
	Total	100.13	1.000

APPENDIX 7

Equations and data used in construction of Figure 15

	log K values at 150°C	Reference
$H_2S = H^+ + HS^-$	-6.66	1
$HS^- = H^+ + S^{2-}$	-11.07	1
$2H^+ + SO_4^= = H_2S + 2O_2$	78.10	2
$HSO_4^- = H^+ + SO_4^=$	-3.79	2
$H_2S + 1/2\ O_2 = H_2O + 1/2\ S_2$	19.68	2
$FeS_2 = FeS + 1/2\ S_2$	-9.98	3
$3FeS_2 + 2O_2 = Fe_3O_4 + 3S_2$	40.30	4
$2FeS_2 + 3/2\ O_2 = Fe_2O_3 + 2S_2$	34.56	4
$3FeS + 2O_2 = Fe_3O_4 + 3/2\ S_2$	70.66	4
$Cu_5\ FeS_4 + 4FeS_2 = 5CuFeS_2 + S_2$	13.29	3
$CuFeS_2 + H^+ + 1/4\ O_2 = FeS_2 + Cu^+ + 1/2\ H_2O$	6.90	5
$CuCl = Cu^+ + Cl^-$	2.48	6
$3KAlSi3O_8 + 2H^+ = KAl_2AlSi3O_{10}(OH)_2 + 2K^+ + 6SiO_2$	10.2	7

Reference

1. Naumov et. al. (1971)
2. Helgeson (1969)
3. Schneeberg (1973)
4. Haas & Robie (1973)
5. Walshe & Solomon (1981)
6. Crerar & Barnes (1976)
7. Shade (1974)